Universidade do Minho
Escola de Ciências da Saúde

Ana Catarina Oliveira Ferreira

Searching for the role of lipocalin-2 in the central nervous system

O papel da lipocalina-2 no sistema nervoso central

Junho 2012

Searching for the role of lipocalin-2 in the central nervous system O papel da lipocalina-2 no sistema nervoso central
Ana Catarina Oliveira Ferreira
UMinho|2012

Universidade do Minho
Escola de Ciências da Saúde

Ana Catarina Oliveira Ferreira

Searching for the role of lipocalin-2 in the central nervous system

O papel da lipocalina-2 no sistema nervoso central

Dissertação de Mestrado
Mestrado em Ciências da Saúde

Trabalho realizado sob a orientação da
Professora Doutora Fernanda Marques
e da
Professora Doutora Joana Palha

Junho 2012

DECLARAÇÃO

Nome: Ana Catarina Oliveira Ferreira

Endereço eletrónico: acoliveira@ecsaude.uminho.pt

Telefone: +351 912884159

Número do Bilhete de Identidade: 13172955

Título dissertação:

Searching for the role of lipocalin-2 in the central nervous system

O papel da lipocalina-2 no sistema nervoso central

Orientadores:

Professora Doutora Fernanda Marques

Professora Doutora Joana Palha

Ano de conclusão: 2012

Ramo de Conhecimento do Mestrado: Ciências da Saúde

Universidade do Minho, Junho de 2012

Assinatura: _____

Aos meus pais

Agradecimentos

A presente dissertação é resultado da minha investigação científica no ICVS, contudo tal não poderia ter acontecido sem ajuda de todos aqueles a quem, abaixo, não posso deixar de expressar a minha maior gratidão.

À Fernanda, por ser sido mais que uma orientadora, uma verdadeira companheira e amiga. Obrigada pelo apoio e presença incondicionais e por acreditar sempre que eu era capaz de chegar até aqui.

À Joana e ao Nuno, pelas diversas discussões científicas e importantes sugestões, pelos desafios propostos e pelo entusiasmo.

Ao João, por ter sido um verdadeiro mentor aquando da minha chegada ao ICVS e por sempre acreditar em mim. Um Muito Obrigada por tudo!

À Falcão, por me saber dar na cabeça no momento certo, por todas as 'discussões', fossem elas de que conteúdo, pela imensa ajuda e por ser uma 'mini-chefe' cheia de energia e boa disposição.

À Ashley e ao Sandro, por partilharem comigo mais do que a inexplicável sensação de cada nova descoberta, a vossa amizade e companheirismo. Obrigada por tudo!

À Susana Roque, Margarida e Nadine, pela partilha de ideias e importantes sugestões.

Aos meus eternos companheiros de carteira, o 'gang' JPêgo: Paula, Ana Rita e António Melo. Obrigada pelas infinitas horas de convívio e descontração, pelas risadas e momentos que só nós sabemos!

Ao Zé Miguel, um obrigado pelas lições de cultura e sabedoria e por me dar a conhecer o Sr. BNST.

À Cristina (Tininha!), à Sofia, à Diana, ao Miguel e à Filipa, um muito obrigada pela partilha desta etapa comigo e pelos imensos momentos de diversão, companheirismo e discussões científicas.

A todos os NeRDs, pelo apoio e sugestões partilhadas e auxílio prestado.

À Pipoca, pela amizade e por me acompanhar nesta e outras etapas.

Aos meus amigos, por nem sempre compreenderem as minhas ausências mas por me apoiarem mesmo assim.

Ao Dinis, pelo apoio incondicional, pela paciência e compreensão, e por todo o carinho e força. Sem ti tudo teria sido bem mais difícil! Obrigada por tudo.

Aos meus pais e avó, por suportarem as minhas muitas ausências sem questionarem, por toda a preocupação e apoio incondicional, pelo amor e exemplo de força. Muito Obrigada!

Searching for the role of lipocalin-2 in the central nervous system

Abstract

Lipocalin-2 (LCN2), a well described secreted protein, has a denotable function as part of the innate immune response. With a remarkable broad expression and rapid induction upon stimulus and in tissues more prone to infection, LCN2 is able to limit bacterial growth through iron-depletion strategies, since it binds iron-loaded siderophores secreted by bacteria during infection. On the other hand, the evidence for the existence of an endogenous mammalian siderophore, along with the capacity for LCN2 to interact with specific cell surface receptors, has brought into light its significance in mediating cellular processes through iron mechanisms, even in basal conditions. In fact, an iron delivery pathway mediated by LCN2 has been proposed with ultimate roles in cell proliferation and survival, tissue development and protection and cellular apoptosis.

However, studies addressing LCN2 involvement in such processes are limited to the periphery, being its role in the central nervous system (CNS) context less explored. In fact, most of the reports show LCN2 importance in an inflammatory context, as an autocrine mediator of reactive astrocytosis or even in the apoptosis and deramification of activated microglia. Additionally, its behavior as an acute-phase protein at the brain barriers adds the involvement of LCN2 in the mechanism of immune defense in brain contexts. However, concerning the role of LCN2 in the physiological brain, there is still a gap that remains unfilled. Therefore, and considering the extensively described functions in the periphery of LCN2 as an iron-traffic protein, we sought to investigate the role of LCN2 in normal brain development and function. Taking advantage of a mouse strain with a target deletion of the *Lcn2* gene (LCN2-null mice), we analyzed the impact of LCN2 in the CNS through behavioral, morphological and cellular approaches. Our findings propose for a putative participation of LCN2 in the development and maturation of specific brain regions related to spatial perception and coordination, whereas in adulthood, LCN2 was observed to trigger altered emotional states, as LCN2-null mice displayed both anxious and depressive-like behaviors. Concomitantly, morphological and cellular approaches evidenced the contribution of LCN2 in the regulation of emotional-related structures, namely the bed nucleus of the stria terminalis (BNST) and in the subgranular zone (SGZ) of the hippocampus. Respectively, LCN2-null mice presented an increased spine density in the BNST and a decreased cell proliferation at the SGZ. Therefore, LCN2 can be assumed to be involved in the modulation of both morphological and cellular mechanisms that, in turn, can culminate with the altered behaviors, namely anxious and depressive-like ones.

O papel da lipocalina-2 no sistema nervoso central

Resumo

A lipocalina-2 (LCN2), descrita como uma proteína secretada, tem uma importante função na resposta imunitária inata. Com uma notável e rápida indução aquando de um estímulo e em tecidos expostos a infeção, a LCN2 é capaz de limitar o crescimento bacteriano através de estratégias de depleção de ferro, uma vez que se liga a sideróforos bacterianos carregados com ferro durante uma infeção. Por outro lado, a existência de sideróforos mamíferos endógenos, juntamente com a capacidade da LCN2 de interagir com recetores na superfície celular, tem revelado a sua importância em mediar processos celulares através do transporte de ferro, mesmo em condições fisiológicas. De facto, uma via do metabolismo do ferro mediada pela LCN2 foi proposta, e consequentemente funções na proliferação celular, no desenvolvimento e proteção de tecidos, assim como na apoptose têm sido mostradas.

Contudo, a maioria dos estudos que demonstram o envolvimento da LCN2 na mediação de tais processos celulares são limitados à periferia, sendo que o seu papel no contexto do sistema nervoso central (SNC) é menos explorado. Aqui, a função da LCN2 tem sido mais demonstrada no contexto da inflamação, como um mediador autócrino da proliferação de astrócitos, e ainda na apoptose e desramificação da microglia ativada. Adicionalmente, o seu comportamento como uma proteína aguda nas barreiras do cérebro acrescenta a sua relevância em mecanismos de defesa do sistema imunitário também no SNC. No entanto, e no que diz respeito à função da LCN2 no cérebro em condições fisiológicas, muito ainda está por descobrir.

Tendo em conta a extensa caracterização na periferia da LCN2 como uma proteína transportadora de ferro, com o presente estudo procurou-se investigar qual o seu papel no normal desenvolvimento e funcionamento do cérebro. Usando como modelo animal um ratinho no qual o gene que codifica para a LCN2 foi removido, analisamos a importância da LCN2 no SNC através de uma análise comportamental, morfológica e celular. Os resultados demonstram o envolvimento da LCN2 na maturação de regiões específicas do cérebro envolvidas na aquisição da perceção espacial e na coordenação, enquanto numa fase adulta, a LCN2 está envolvida no desencadeamento de comportamentos emotivos, nomeadamente ansiosos e depressivos. Simultaneamente, a análise morfológica e celular evidenciam a contribuição da LCN2 na modulação destes processos em estruturas relacionadas com processos emotivos, nomeadamente no núcleo da estria terminal e na zona subgranular do hipocampo. Nestas regiões foi verificado que os animais nos quais o gene *Lcn2* foi removido apresentam um aumento significativo de densidade de espinhas nos neurónios do núcleo da estria terminal e uma diminuição no total da proliferação celular no hipocampo. Consequentemente, podemos assumir que a LCN2 está envolvida na modulação de ambos processos morfológicos e celulares, os quais, por sua vez, culminam nas alterações comportamentais verificadas, nomeadamente na ansiedade e depressão.

TABLE OF CONTENTS

Abbreviations

ANGD	Anogenital Distance
AS	Acoustic Startle
BBB	Blood Brain Barrier
BCSFB	Blood-Cerebrospinal Fluid Barrier
BLA	Basolateral Amygdala
BNST	Bed Nucleus of the Stria Terminalis
BrdU	Bromodeoxyuridine
BSA	Bovine Serum Albumin
CNS	Central Nervous System
CP	Choroid Plexus
CSF	Cerebrospinal Fluid
DAB	3,3'-Diaminobenzidine Substrate
DG	Dentate Gyrus
DNA	Deoxyribonucleic acid
EPM	Elevated Plus Maze
FST	Forced Swim Test
HCl	Hydrochloric Acid
Hetero	Heterozygous
HPA	Hypothalamic-Pituitary Adrenal
H_2O_2	Hydrogen Peroxide
LCN2	Lipocalin-2
LPS	Lipopolysaccharide
MWM	Morris Water Maze
NaCl	Sodium Chloride
Neo	Neomicin
NGAL	Neutrophil Gelatinase Associated Lipocalin
OF	Open Field
PCR	Polymerase Chain Reaction
PFA	Paraformaldehyde
PFC	Prefrontal Cortex
PND	Postnatal Day
RAM	Radial Arm Maze
RMS	Rostral Migratory Stream
SEM	Standard Error of the Mean
SEZ	Subependymal Zone
SGZ	Subgranular Zone
TBS-T	Tris Buffer Saline-Tween
Wt	Wild-Type

Figures Index

Tables Index

CHAPTER 1 - INTRODUCTION

1.1 Iron homeostasis

Iron is a required and an essential element for fundamental biological processes. As part of enzymes, cytochromes and protein prosthetic groups, iron ensures cellular homeostasis, participating in processes that range from cell proliferation and survival to oxygen transport and energy metabolism (Hentze et al., 2004; Mesquita et al., 2012). Although essential, systemic iron imbalance, whether due to its deficiency or excess, can lead to the development of several pathological conditions, such as anemia, or iron deposition as in hemacromatosis and in some neurodegenerative disorders (i.e. Alzheimer's and Parkinson's diseases) (Mesquita et al., 2012).

Of interest, there is no biological mechanism to excrete iron from the body, apart from physiological bleeding in women and enterocyte renewal. Therefore, iron levels are tightly controlled at the absorption level. The liver assumes the control of this regulation through the production of a small peptide, hepcidin, (Krause et al., 2000)that in turn binds to ferroportin on the surface of the enterocytes, causing its internalization and degradation; this ultimately leads to a decrease in iron absorption to the bloodstream (Anderson and Frazer, 2005). In the blood, iron is mostly bound to plasma proteins, particularly to transferrin, responsible for both the transport and delivery of iron into the majority of cells (Gomme et al., 2005). After binding to receptors (mainly transferrin receptor 1), transferrin enters an endocytic pathway and, within endosomes, iron dissociates from the receptor and is transported into the cell cytoplasm where it can be stored bound to ferritin (Harrison and Arosio, 1996).

In the central nervous system (CNS), the mechanism through which iron homeostasis is regulated is less known, but must be specific and precise since when iron accumulates in peripheral organs, such as in the case of hemacromatosis, the brain seems spared.

The brain parenchyma is protected from the blood content by two main barriers, the brain-blood barrier (BBB) and the blood-cerebrospinal fluid barrier (BCSFB). Both have been showed to mediate iron uptake into the brain through transferrin-mediated endocytosis (Moos et al., 2006). Once inside the endothelial cell of the BBB or the choroid plexus (CP) epithelial cell of the BCSFB, iron is released through ferroportin into the interstitial fluid of the brain parenchyma, or to the cerebrospinal fluid (CSF), respectively, where it binds to transferrin and is taken up by neurons and glia cells

(Moos et al., 2006). Interestingly, the CP has been recently suggested to play a specific role in regulating brain iron homeostasis, at least in particular circumstances such as in response to peripheral inflammation, where the CP is able to produce and secrete hepcidin (Marques et al., 2009).

Of notice, it is well known that both in the periphery and in the CNS, transferrin is considered the main route through which cells acquire most of their iron. However, studies with transferrin deficient mice demonstrated that the transferrin pathway is not essential for the delivery of iron to many tissues (Garrick and Garrick, 2009). These mice present anemia, deficiency in the development of the CNS and iron accumulation in the liver, but most of the epithelial organs have normal iron levels (Yang et al., 2002).

All together, these observations support the existence of alternative pathways for iron delivery to cells. One of such putative mechanisms may be mediated by lipocalin-2 (LCN2). This 25 kDa protein from the lipocalin protein family (Flower et al., 2000) has been considered an iron-related protein given its ability to sequester bacterial iron-loaded siderophores secreted by bacteria during infection (Flo et al., 2004). As such, LCN2 participates in the innate immune response by depleting iron from the invading microorganisms. However, in light of the recent discovery of an endogenous mammalian siderophore (Bao et al., 2010; Devireddy et al., 2010), LCN2 may, as well, bind, transport and delivery iron to cells through its membrane receptor.

In the next sections we will explore the role and putative functions of LCN2 on both basal and pathological conditions in the periphery and in the CNS.

1.2 The lipocalin protein family

LCN2 (also known as 24p3, neutrophil gelatinase-associated lipocalin (NGAL), oncogene 24p3, or siderocalin) belongs to the lipocalin protein family, a large and diverse group of small (160-180 residues in length) soluble and often secreted proteins present across species. A remarkable feature of this family is the great diversity of the primary sequence of its proteins, with an unusually low level of overall sequence conservation, in some case as low as 20% (Flower, 1994; Grzyb et al., 2006). However, membership of this family has been largely identified based on structural similarities as they all share a common secondary and tertiary structural feature - called as the "lipocalin fold", a cup-shaped cavity that can bind to specific ligands (Flower et al.,

2000). This conformation has allow them to be carriers, transporting predominantly small lipophilic molecules such as steroids, bilins, retinoids and lipids, to form complexes with soluble macromolecules and to bind specific cell-surface receptors (Flower, 1996). In fact, lipocalins are described to participate in the regulation of cell division, differentiation and cell to cell adhesion and survival and in the modulation of the immune response (Flower, 1996; Flower et al., 2000; Chakraborty et al., 2012).
As member of this lipocalin protein family, LCN2 (lipocalin product of a single gene, the *24p3*), is believed to also engage some of the overall functions described for lipocalins. Its emerging evidence as a significant mediator of several physiological and pathological processes has caught our attention.

We will, therefore, consider the major key features of LCN2 in detail.

1.3 LCN2 – where and when?

When first described as component of human neutrophils, LCN2 sequence did not match with any known human protein, but instead showed a high degree of similarity with the deduced sequence of the rat α-2-microglobulin-related protein and the mouse protein 24p3, that in turn also belong to the lipocalin family (Kjeldsen et al., 1993; Kjeldsen et al., 1994).
Originally with no function described, LCN2 was found stored in specific human neutrophil granules and co-localizing with lactoferrin as a monomeric and homodimeric form. In addition, its covalent association with the 92-kDa monomeric form of matrix metalloproteinase-9 (MMP-9), a gelatinase secreted by neutrophils for extracellular matrix degradation and remodeling (Kjeldsen et al., 1993; Kjeldsen et al., 1994), led to be named as neutrophil gelatinase-associated lipocalin (NGAL) (Kjeldsen et al., 1993; Kjeldsen et al., 1994).
Afterwards, it was also found in mouse neutrophils (Kjeldsen et al., 2000), although the first reports in murine models were in BALB/c 3T3 fibroblasts upon stimulation (Nilsen-Hamilton et al., 1982) and as a gene highly induced during the transition of mouse kidney cells from a quiescent to a proliferative state, as a result of virus infection (Hraba-Renevey et al., 1989). Meanwhile, several expression studies described LCN2 to be present in tissues that are more prone to exposure to infection and highly secreted by mucus producing epithelial cells of the respiratory tract (lung and trachea) (Cowland and Borregaard, 1997; Friedl et al., 1999). Other major sites of LCN2 expression

described are blood and peritoneal cells (Flo et al., 2004), macrophages (Meheus, 1993), endothelial (Liu and Nilsen-Hamilton, 1995) and epithelial cells (Marques et al., 2008).

While present in normal tissues, mainly the kidney and thymus, both in humans and mice (Friedl et al., 1999), LCN2 is mainly expressed in response to stimuli. Among these, lipopolysaccharide (LPS) has been shown to be the major inducer of LCN2 expression. For instances, cultured murine macrophages when stimulated with LPS where shown to highly express LCN2 (Meheus, 1993), which was also reported to occur in primary cultures enriched in CP epithelial cells (Thouvenot et al., 2006). These *in vitro* studies were largely confirmed by posterior *in vivo* data, where in conditions of a peripheral immune challenge by LPS, LCN2 was shown to behave as an acute-phase protein in the CP epithelial cells (Marques et al., 2008). Importantly, and accompanying such quick up-regulation in the CP, LCN2 protein levels were also found elevated in the cerebrospinal fluid (CSF), which is mainly produced by the CP; and in blood vessels of the brain parenchyma (Marques et al., 2008). LCN2 had also been claimed as a liver acute-phase protein in response to the *in vivo* injection of turpentine (Liu and Nilsen-Hamilton, 1995), and at the lungs after LPS stimulus (Sunil et al., 2007).

Similarly, *in vitro* stimulation of mouse liver cells (Liu and Nilsen-Hamilton, 1995), L-cells (Garay-Rojas et al., 1996) and primary thymocytes (Devireddy et al., 2001) with dexamethasone induces the acute expression of LCN2 (Liu and Nilsen-Hamilton, 1995). This regulation of expression is mainly explained by the described existence of two glucocorticoid responsive core elements (GRE) in the *24p3* gene promoter (Garay-Rojas et al., 1996). Additionally, pro-inflammatory cytokines were also shown to be able to induce the constitutively expression of LCN2 in epithelial inflamed lungs (Cowland et al., 2003). This induction was observed by interleukin-1β (IL-1β) but not by TNF-α stimulation (Cowland et al., 2003) and further work provided the evidence for LCN2 induction by TNF-α only in the presence of IL-1β (Karlsen et al., 2010).

Overall, a striking observation in the study of LCN2 expression is its strong induction (both mRNA and protein) in different cell lines and tissues following exposure to a variety of stimuli and a number of inducers have been identified, thus retrieving LCN2 with major functions in defense mechanisms and in a variety of inflammatory responses (reviewed at (Borregaard et al., 1995)).

1.4 LCN2 ligands

Lipocalins are characterized by their ability to bind different lipophilic substrates and, if some bind several ligands, others are specific for a single one (Kjeldsen et al., 2000). Early studies hypothesized LCN2 to have an immunomodulatory activity by binding and clearing lipophilic mediators of inflammation such as the neutrophil chemoattractant *N*-formyl-Met-Leu-Phe (fMLP) (Allen et al., 1989; Sengelov et al., 1994), the platelet activating factor, leukotriene B4, and LPS (Nielsen et al., 1996). However, unlike other lipocalins, LCN2 binding cavity was shown by both X-ray crystallography (Goetz et al., 2000) and nuclear magnetic resonance spectroscopy (Coles et al., 1999) to be distinct as it is unusually large and atypically polar. In fact, the relative low affinity of LCN2 for *N*-formyl tripeptides was shown, suggesting that any of the previous proposed hydrophobic ligands are unlikely to be the preferred ligands for LCN2 (Goetz et al., 2000).

Goetz and colleagues (2002) identified the ability of LCN2 to bind negatively charged catecholate-type ferric bacterial siderophores, small molecules produced during bacterial infection to scavenge iron from the host that have higher affinity to iron than the host iron-binding proteins (Goetz et al., 2000; Goetz et al., 2002). In this work, LCN2 was shown to be able to bind iron loaded bacterial siderophores in its binding pocket but, unlike lactoferrin or transferrin, LCN2 could not bind positively charged iron ions alone, being specific only for iron already earmarked for bacterial use by siderophores complexes (Goetz et al., 2002).

Classically, lipocalins derive their name from the ligand that they bind. Therefore, at this point the authors proposed LCN2 to be renamed siderocalin based on the ligand it binds (Goetz et al., 2002).

Importantly, LCN2 is now described to be able to bind a wide variety of siderophores thus mediating its physiological role as a broad specificity siderophore binding protein and most of its described functions have been inferred from these binding capacities.

1.5 LCN2 major functions

By the time it was first reported (Nilsen-Hamilton et al., 1982; Hraba-Renevey et al., 1989), LCN2 was suggested to be involved in the control of cell regulation, in normal and/or transformed cells, possibly through the transport of lipophilic molecules (Flower, 1994). The following description of LCN2 expression in neutrophils and tissues exposed to microorganisms and in conditions of inflammation/infection has brought the

possibility of an antimicrobial activity for LCN2 (Kjeldsen et al., 2000) or even a role in inflammation or cellular growth (Kjeldsen et al., 2000). Its capacity to bind bacterial catecholate-type ferric siderophores (Goetz et al., 2002), confirmed the suggestion of LCN2 as a potent bacteriostatic agent that participates in the iron-depletion strategy of the innate immune system. Of interest, the identification of endogenous mammalian siderophores (Bao et al., 2010; Devireddy et al., 2010) along with the capacity of LCN2 to interact with specific cell-surface receptors raised the possibility that LCN2 participates in iron trafficking and metabolism (Yang et al., 2002; Devireddy et al., 2005). Therefore, among other putative described functions, LCN2 major roles reported so far are in relation to the innate immune response and the intracellular iron trafficking. These and other functions that have been attributed to LCN2 will now be described in detail.

1.5.1 The role of LCN2 in the innate immune response

Upon an infection, microbes, chiefly bacteria, require iron for growth and proliferation and have evolved strategies to survive within the severely iron-poor environment of the human body. The exceedingly low availability of free iron is attributable to iron-binding proteins such as transferrin, which form complexes with any available free iron molecules. To cope with their need, bacteria acquire most of their iron from the host by synthesizing siderophores, low molecular weight proteins that scavenge iron from the various host iron-binding proteins and transport it into the pathogen (Ratledge and Dover, 2000). Interestingly, siderophores have an affinity for iron several times higher than that of the host endogenous iron carrier proteins (Ratledge and Dover, 2000).

In this context, Goetz and colleagues (2002) have shown, *in vitro*, that LCN2 has a high affinity for bacterial siderophores, both in their iron-loaded and iron-free states, and that it even competes with the pathogen for iron, thus limiting the bacteria propagation (Goetz et al., 2002) (Figure 1). Upon this discovery, LCN2 was immediately suggested to be involved in the innate immune response: LCN2 was assumed to be released by neutrophils at sites of infection and inflammation to sequester bacterial siderophores, thus participating in the antibacterial iron-depletion strategy of the innate immune response (Goetz et al., 2002).

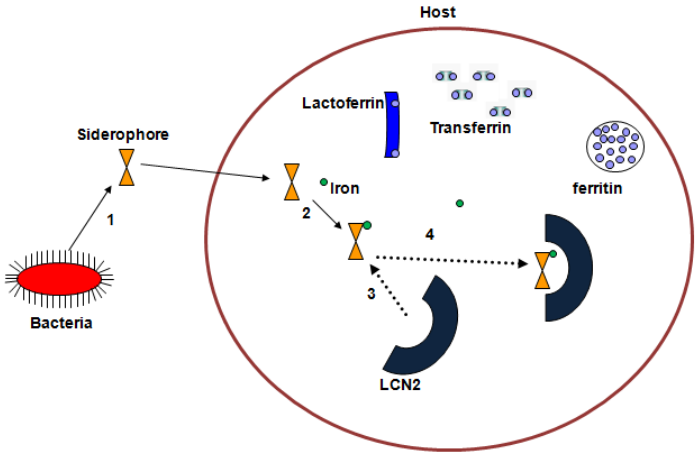

Figure 1: *Schematic representation addressing how bacteria acquire iron from the host*. Upon infection, bacteria synthesize siderophores (1) to scavenge iron from host iron-binding proteins (transferrin, lactoferrin and ferritin) for its growth and proliferation (2). In response, the host produces LCN2 that is able to bind iron-loaded siderophores (3) thus limiting the availability of iron for bacterial growth (4).

In this response, LCN2 is induced through the activation of Toll-like receptors (Flo et al., 2004). Studies using mice with a target deletion of *Lcn2* gene (LCN2-null) revealed that under pathogen-free conditions, there is no major phenotype present; however, upon exposure to sublethal doses of *Escherichia coli* H9049, LCN2-null mice were far more likely to develop bacteraemia (Flo et al., 2004). The absence of the defense mechanism mediated by LCN2 can lead to sepsis and death (Flo et al., 2004) extolling LCN2 with an essential bacteriostatic role (Berger et al., 2006).

Holmes and colleagues (2005) showed LCN2 to be also able to bind soluble siderophores of mycobacterium, including *Mycobacterium tuberculosis* (Holmes et al., 2005), and other studies reported the up-regulation of LCN2 in primary cultured macrophages in response to *Salmonella* (Nairz et al., 2009) and in the respiratory tract in response to colonization by *Klebsiella pneumoniae* (Nelson et al., 2005; Chan et al., 2009).

Of interest, LCN2 may similarly protect the brain from invading microorganisms, since its expression occurs at the both barriers of the brain: in the epithelial cells of CP in the CP-CSF barrier and by the endothelial cells of the capillaries that irrigate the brain parenchyma in the blood-brain barrier (Marques et al., 2008). The authors hypothesized that on one hand, LCN2 might reduce iron access to the bacteria in the blood vessels and, in the case of bacteria entering into the CSF, CP-borne LCN2 can sequester siderophore-bound iron and prevent bacteria dissemination within the ventricular brain system and brain parenchyma (Marques et al., 2008).

LCN2 is, therefore, described as an accurate mechanism of sensing microbial metabolism to modulate the host response appropriately, assuming iron an important role in such modulation.

1.5.2 LCN2 mechanism of action in iron delivery

The delivery of iron to cells is essential for cell growth and development and most cells acquire iron by capturing iron-loaded transferrin (Garrick and Garrick, 2009). The importance of LCN2 in iron-related processes emerged upon its identification as an inducer of rat metanephric mesenchyma conversion into epithelia through associations with iron (Yang et al., 2002). Remarkably, the authors were able to show that the LCN2 expressed in mammalian kidney contains iron, and even that LCN2 is able to deliver iron into cells through a mechanism independent of transferrin (Yang et al., 2002). This alternative pathway was described to require endocytosis and endosomal acidification and the modulation of iron-responsive genes by LCN2: enhancement of transferrin expression and reduction in the expression of the transferrin receptor 1 (Yang et al., 2002). Moreover, the internalization of either transferrin or LCN2 was dependent of the kidney developmental phase, with earlier epithelial progenitors incorporating LCN2 while the further staged epithelial cells internalized mainly transferrin (Yang et al., 2002). As a whole, data from these authors showed LCN2 as an iron-donor protein with functions distinct from those of transferrin, vital for early embryonic development, at least in the kidney (Yang et al., 2002).

These observations were striking given that LCN2 does not have an intrinsic ability to bind iron, but instead to bind iron-loaded siderophores (Goetz et al., 2002). However, the recent description for the existence of an endogenous mammalian siderophore has brought into light the possibility for a physiological-relevant mechanism of iron uptake mediated by LCN2 (Bao et al., 2010; Devireddy et al., 2010). While bacterial siderophores are not synthesized by mammalian cells, they are composites of well known functional groups such as hydroxybenzoates and hydroxybenzenes that were found in a variety of compounds in mammalian serum and urine, where interestingly LCN2 traffics (Bao et al., 2010), thus suggesting that it might bind those compounds (Bao et al., 2010). In fact, through the use of mouse and human aseptic urine as a source to search for novel LCN2 ligands and through structural analyses, it was identified a subset of catechols that bind both iron and LCN2, revealing a novel mechanism of iron capture and release (Bao et al., 2010; Devireddy et al., 2010).

In accordance, Yang and colleagues (2002) have described that following the cellular uptake of LCN2 by endocytosis, the bound iron is released leading to an increase in intracellular iron concentrations (Yang et al., 2002). These internalization mechanisms of the secreted LCN2 suggested the existence of cellular receptors. In fact, megalin (Hvidberg et al., 2005) and the solute carrier family 22 (organic cation transporter), member 17 (SLC22A17) also known as brain-type organic cation transporter (generally named as 24p3R) (Devireddy et al., 2005) are the two known receptors described to allow LCN2 to engage roles in trafficking iron in and out of the cells.

Megalin, a multi-ligand endocytosis receptor member of the low density lipoprotein receptor family expressed in epithelia, is also known to bind the mouse lipocalins retinol-binding protein and α-2-microglobulin (Hvidberg et al., 2005). Hvidberg and collegues (2005) in their studies reported that both iron-loaded-LCN2 (holo-LCN2) and iron-lacking LCN2 (apo-LCN2) were able to bind megalin with high affinity, thus leading to LCN2 endocytosis (Hvidberg et al., 2005). Moreover, its tissue expression was found to be coincident with the induction of LCN2 expression during inflammation, thus highlighting megalin as an endocytic receptor capable of binding iron transporting LCN2 and mediating its uptake (Hvidberg et al., 2005). The relevance of megalin in regulating iron levels through LCN2 became evident when megalin-null mice were described to have a significantly higher urine excretion of LCN2 (Mori et al., 2005).

With respect to 24p3R, it was shown that LCN2 may be internalized whether in its apo- or holo- forms, in this way being able to modulate both iron uptake and excretion from cells (Devireddy et al., 2005). Indeed, a pathway for LCN2-mediated iron depletion has been proposed, where the iron status of LCN2 is the critical determinant of its activity (Figure 2) (Devireddy et al., 2005). Briefly, holo-LCN2 binds to 24p3R, is internalized, and releases its bound iron, thereby increasing intracellular iron concentration and preventing apoptosis; by contrast, apo-LCN2 when internalized, chelates iron and transfers it to the extracellular medium, thereby leading to iron efflux that results in apoptosis and cell death, mediated by the pro-apoptotic Bcl-2-interacting mediator of cell death (Bim) (Devireddy et al., 2005; Richardson, 2005) (Figure 2).

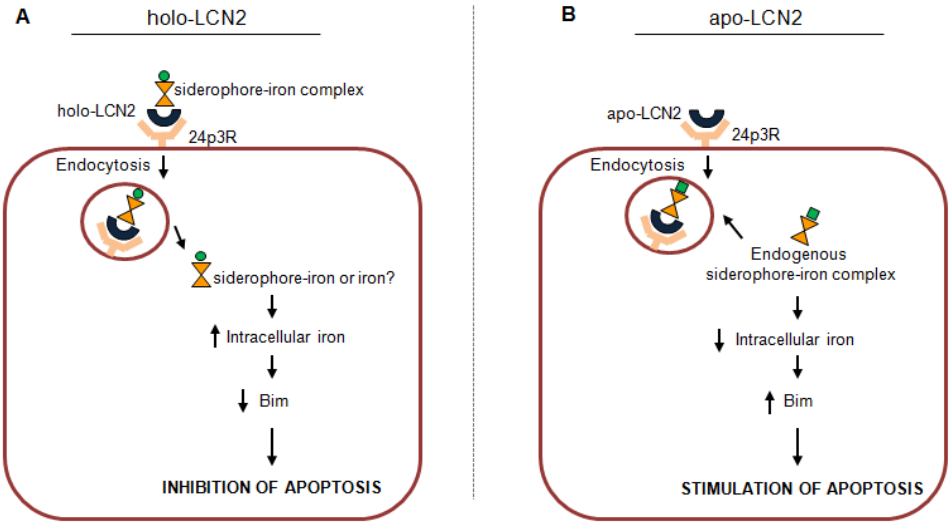

Figure 2: *Possible effects of holo and apo-LCN2 on iron metabolism and apoptosis, mediated by 24p3R.* (A) Holo-LCN2 containing iron bound to the siderophore donates iron to cells via the 24p3R. Upon internalization of the LCN2-receptor complex, iron is removed, leading to an increase in the intracellular levels of iron. This accounts for the prevention of cell apoptosis through the decrease in the expression of the pro-apoptotic protein Bim. (B) Apo-LCN2 binds to 24p3R and is also internalized into the cell. Once inside, it is suggested to putatively become complexed with an endogenous siderophore, forming the holo-LCN2. Its subsequent release from the cell by exocytosis leads to a depletion of iron from the cell resulting in the upregulation of the pro-apoptotic molecule Bim and, therefore, stimulation of apoptosis (Adapted from (Richardson, 2005)).

In summary, the isolation and identification of the endogenous mammalian siderophore, together with the existence of receptors for LCN2, has brought into light the additional biological relevance of LCN2 in iron delivery mechanisms in basal conditions.

This may explain several of the reports on the role of LCN2 in cellular processes. In fact, LCN2 has been shown to regulate cell division (Gwira et al., 2005), differentiation and maturation during development (Yang et al., 2002) and epithelial morphogenesis (Yang et al., 2002; Schmidt-Ott et al., 2007) and also to contribute in the homeostasis of hematopoietic cells lineages due to its ability to induce apoptosis (Liu et al., 2011).

Of interest, is the evidence that LCN2 may be either protective/pro-survival (Mishra et al., 2004; Mori et al., 2005; Roudkenar et al., 2009), or pro-apoptotic (Kehrer, 2010), which, as well, may depend on whether LCN2 is depleting or delivering iron from or to cells.

In this context, this has been evidenced in kidney injury situations, where LCN2 has been shown to be up-regulated for protection (Mishra et al., 2004; Mori et al., 2005).

Also of interest is the variable described contribution of LCN2 in cancer, since both cancer promoting (Bolignano et al., 2010; Kehrer, 2010) and anti-tumoral (Jin et al., 2011) actions have been reported.

Additionally, and also controversial, is the role of LCN2 as a putative adipokine, where LCN2 has been suggested as a marker of obesity (Li and Chan, 2011), but with a precise role in glucose and insulin homeostasis still to be clarified (Guo et al., 2010; Law et al., 2010; Jun et al., 2011).

1.6 LCN2 at the central nervous system

The evidence for a role for LCN2 in cell homeostasis, through iron, has increased the search of knowledge regarding its involvement in several contexts and distinct organs. Despite its implication in several cellular processes, little is known about LCN2 and the CNS, particularly with respect to normal brain physiology.

Of interest, the literature is still not conclusive concerning the sites of LCN2 synthesis in basal conditions, with recent reports showing immunostaining and mRNA expression in specific brain regions of the adult rat, namely the olfactory bulb, brainstem and cerebellum (Chia et al., 2011).

The first reports regarding LCN2 in the CNS described its up-regulation in whole brain homogenates in response to inflammation induced by turpentine injection (Liu and Nilsen-Hamilton, 1995), and later in the mouse brain after focal ischemia (MacManus et al., 2004) and in spinal cord injury (De Biase et al., 2005).

Also in response to an inflammatory status, LCN2 was shown to be expressed in astrocytes from different brain regions (striatum, cerebral cortex, hippocampus and cerebellum) (Lafon-Cazal et al., 2003) and, nowadays it is broadly accepted and described that astrocytes are the main brain cells expressing LCN2.

Interestingly, both *in vitro* and *in vivo* approaches have shown the expression of LCN2 upon the LPS stimulus at the CP epithelial cells (Thouvenot et al., 2006; Marques et al., 2008; Ip et al., 2011), from where it is secreted into the CSF (Marques et al., 2008). Of notice, LCN2 was not detected at the CP in basal conditions but only in response to the stimulus (Marques et al., 2008; Ip et al., 2011).

Most remarkably is the recent report that the 24p3R receptor for LCN2 is constitutively expressed by the mouse brain and that its levels of expression are not affected by systemic LPS administration (Ip et al., 2011). Additionally, differences between the basal expression of LCN2 and 24p3R mRNA were noticed. While 24p3R mRNA levels

were only detected in neurons and in the CP upon the LPS stimuli, endothelial, astrocytes, microglia cells as well as the CP, but not neurons, were identified as the main cellular sources for LCN2 mRNA in the CNS (Ip et al., 2011). As a whole, LCN2 was reported to be strongly produced in the CNS by LPS inflammatory stimulus and that neurons seem to be the target for the actions of LCN2 as the expression of the 24p3R assembles (Ip et al., 2011).

Even though the cellular functions of LCN2 in the CNS remain enigmatic, some new insights have been given by Lee and colleagues that through *in vitro* studies showed that after inflammatory stimulation of cultured astrocytes, LCN2 expression and secretion was increased and, most importantly, was critical in inducing cell death sensitization, stimulation of cell migration and morphological changes of reactive astrocytes (Lee et al., 2009). Consequently, LCN2 was proposed to be an autocrine mediator of reactive astrocytosis, a process in which astrocytes when responding to injury become hypertrophic and proliferate (Lee et al., 2009). Most remarkably was the evidence for the involvement of iron metabolism and Bim protein in this LCN2-induced cytotoxic sensitization. At last, these described roles were also confirmed *in vivo* using a zebrafish model (Lee et al., 2009). Of notice, it was shown that LCN2' mediating processes is not restricted to reactive astrocytes since it was demonstrated that LCN2 has also a dual role on both apoptosis and deramification of the *in vitro* activated microglia and, recently, in neuronal cell death, again through the Bim protein activation (Lee et al., 2007; Lee et al., 2012). Recently, it was also described how LCN2 is able to promote cellular migration through the up-regulation of chemokines in the brain (Lee et al., 2011). Using animal models of inflammation, LCN2 was shown *in vivo* to act as a chemokine inducer that once secreted in conditions of inflammation, induces CNS cells to secrete chemokines that amplify the neuroinflammation response by recruiting additional cells (Lee et al., 2011).

In addition, several reports have been linking the described patterns of LCN2 expression and cellular modulation with neurological conditions and states, such as neurodegenerative disorders. For instances, LCN2 was described to be highly expressed in the plasma of patients suffering from mild cognitive impairment (MCI), when compared to healthy control subjects and even to the Alzheimer's Disease (AD) patients (Choi et al., 2011). Contrarily, Naudé and colleagues (2012) report that LCN2 levels in the serum of patients with MCI are not significantly elevated, but describe for the

presence of decreased levels of LCN2 in CSF of human patients with both MCI and AD (Naude et al., 2012). Additionally, and when analyzing the levels of LCN2 in AD human postmortem brain tissues, it was found to be ubiquitously expressed throughout the brain but significantly increased in brain regions associated with AD pathology (hippocampus and entorhinal cortex) (Naude et al., 2012). Previously, Wu and colleagues (2006) had showed that LCN2 mRNA levels were strongly up-regulated in the cortical tissue from AD model mice, both prior or after amyloid-β deposition, one of the hallmarks of AD (Wu et al., 2006).

Also recently, LCN2 was associated to the experimental autoimmune encephalomyelitis (EAE) murine model of multiple sclerosis, since it was found to be up-regulated in the spinal cord at the onset phase of the disease, being predominantly expressed, in this context, by astrocytes and monocytes, along with its receptor (Berard et al., 2012). The role of LCN2 in this disease was evidenced by the increased severity of EAE in the LCN2-null mice (Berard et al., 2012).

An additional field where LCN2 has also been implicated is in the response to stress, which may be related to the presence of glucocorticoid-responsive elements in its gene (Garay-Rojas et al., 1996). Studies in LCN2-null mice exposed to a restraint stress suggest a role for LCN2 in the control of dentritic spine density and maturation, neuronal excitability and anxiety (Mucha et al., 2011).

Finally, and also recently, both in models of spinal contusion injury (Rathore et al., 2011) and of inflammatory pain (Poh et al., 2012) increased expression of LCN2 was described, in both cases attributed to infiltrating neutrophils. In the case of the spinal cord injury model, also astrocytes and neurons were shown to strongly express LCN2 (Rathore et al., 2011).

Altogether, while the participation of LCN2 seems also to be present in the brain in response to injury, little is known on its function in physiological conditions, which is the aim of the present project.

1.7 Research objectives

It is clear that despite all the described features for LCN2, regardless of the context, it is in the CNS that much information is still lacking. The need for understanding LCN2' role in the physiological brain as brought us to this project where we aim to unravel its putative roles during development and in adulthood. To asses this, and taking advantage of mouse model with targeted deletion of *Lcn2* (LCN2-null mice), three major aims were proposed:

1. Explore the role of LCN2 in the normal CNS development and adult function

2. Analyze the morphological brain cytoarquitecture of LCN2-null mice

3. Assess the impact of LCN2 on the proliferative profile of adult neural stem cells

With this project, we expect to contribute to characterize the role of LCN2 in brain function and in behavior.

2.1 Animals

A mouse strain with a targeted deletion of the gene for LCN2 (LCN2-null mice) and their respective wild-type (Wt) and heterozygous (Hetero) littermates were used in all the studies performed.

This LCN2-null mouse strain was generated by deleting the entire coding sequence (Exons 2 to 5) and replacing it by a neomicin (Neo) cassette (Figure 3).

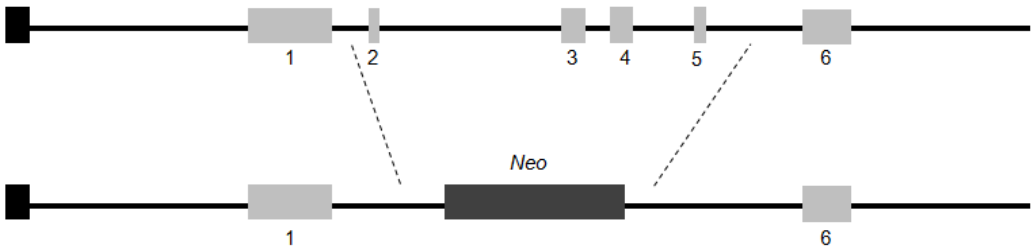

Figure 3: *Generation of LCN2-null mice.* The entire coding sequence (from exons 2 to 5, light grey boxes) were deleted and replaced by a neomycin (Neo) cassette (dark grey box).

All experiment procedures were conducted in accordance with the Portuguese national authority for animal experimentation, *Direcção Geral de Veterinária* (ID: DGV9457). Animals were kept and handled in accordance with the guidelines for the care and handling of laboratory animals in the Directive 2010/63/EU of the European Parliament and of the Council. Efforts were made to minimize the number of animals used and their suffering.

All mice were given standard diet (4RF25 during gestation and postnatal periods, and 4RF21 after weaning; Mucedola SRL, Settimo Milanese, Italy) and water *ad libitum*, with exception to the privation periods that occurred whenever the experiment required so. Animals were maintained under standard laboratory conditions on a 12/12-h light/dark cycle (lights on at 8 a.m.) with an ambient temperature of 21±1ºC and relative humidity of 50-60%.

Matings were prepared for animal colony maintenance: Wt and LCN2-null mice were bred to obtain LCN2-Hetero mice, which in turn were mated. This allowed the production of Wt, Hetero and LCN2-null mixed litters that were used to perform all the studies. Whenever a birth occurred, animals were kept untouched in the home cage with

their mothers until weaning was performed at 21 days of age; males and females were then separated and kept in independent cages, in groups of three to five animals per cage until genotype determination was performed.

Our animals were raised in a BALB/c background and used for most of the experiments, but we also had available the same construct in the C57BL/6 background that we used for cognitive assessment.

2.2 Genotyping

Routinely, mice genotype was confirmed by polymerase chain reaction (PCR). For that, DNA extraction strategies included ear/toe or tail digestions with a Finnzymes´ Phire® Animal Tissue Direct PCR Kit (BioLabs, New England, UK) designed to perform PCR directly from non-fixed animal tissue samples with no prior DNA purification. The process was executed accordingly to the manufacture's instruction. Briefly, the tissue was directly placed into 10 µl of a Dilution Buffer, and 0.5 µl of DNARelease™ Additive for 5 min at room temperature. After an incubation of 2 min at 98ºC, samples were centrifuged and the supernatant containing the DNA quantified using the NanoDrop spectrophotometer (NanoDrop Technologies, Inc., ThermoScientific, Wilmington, USA).

PCR strategy relied on the amplification of the junction of the inserted cassette with the target gene flanking sequences, as in Figure 4. For the detection of both mutated and Wt alleles, two independent pairs of primers, neo1500 and Wild-type, were respectively used (Table 1).

Table 1: Primers sequence for mice genotyping.

Primer Abbreviation	Sequence	TM (ºC)
neo1500	5'-ATCCGGTTCTATCGCCTTCTTGACGAG-3'	
Wild-type	5'-GTCCTTCTCACTTTGACAGAAGTCAGG-3'	58ºC
Common	5'-CACATCTCATGCTGCTCAGATAGCCAC-3'	

TM: Temperature of Melting (ºC)

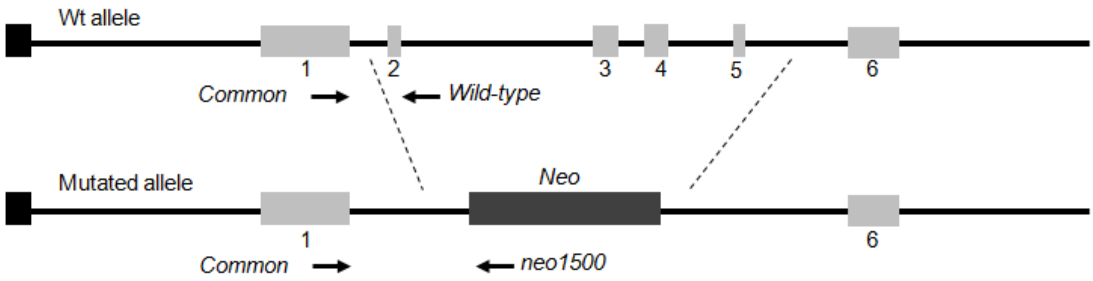

Figure 4: *Schematic representation of the genotype strategy for LCN2-null mice.* The exons are numbered and identified in light grey. Primers *Common* and *Wild-type* were used to amplify the Wt allele, whereas *neo1500* in conjunction with the *Common* primer was used to identify the mutated allele, both with 500 bp.

The *Common* primer is specific for the *Lcn2* gene and, in combination with either *neo1500* or *Wild-type* primers allows to distinguish the LCN2-null mice from the Wt, respectively. Two independent PCR mixtures were required since the product size in both sets of primers is of 500 bp. For each PCR reaction, 1 µl of DNA (100 ng/µl) was used for a final volume of 20 µl of PCR reaction, using the mix and reaction conditions as described in Table 2:

Table 2: PCR Mix composition and reaction conditions.

Master Mix (20 µl)	Volume (µl)	DNA Template	PCR conditions
H_2O (Milli_Q)	14.5		
Taq Buffer (with $(NH_4)_2SO_4$)[1]	2.0		95ºC 2’
$MgCl_2$ (25 mM)	1.2		95ºC 1’
dNTPs (10 mM)	0.4	1 µl (100 ng/ µl)	58ºC 45” 30 cycles
Common (10 µM)	0.4		72ºC 1’
neo1500 (10 µM)	0.4		72ºC 5’
Wild-type (10 µM)	0.4		4ºC ∞
Taq Polymerase (5 U/ µl)[1]	0.1		

[1]Fermentas Life Science, California, USA

The amplified PCR products were separated in a 2% agarose gel stained with ethidium bromide.

2.3 Behavioral assessment

To explore the role of LCN2 in the normal CNS development and function, we evaluated the impact of the absence of this protein through a behavioral characterization both during postnatal development and in adulthood.

One cohort of animals from two independent litters was submitted to a set of behavioral paradigms through the first 21 days of life, to evaluate the acquisition of neurological hallmarks during brain development, the called developmental milestones protocol. Other set of animals from three independent group of litters was assessed for their behavior in adulthood (2-3 months old), which included general evaluation of motor, emotion and cognitive dimensions.

At the end of the experiments, all animals were sacrificed.

Both protocols were replicated at least twice.

2.3.1 Developmental milestones

Assessment of neurobehavioral neonatal development included the execution of a range of well-described tests used to evaluate neurologic parameters such as motor, reflexes and strength/coordination development (Hill et al., 2008; Lim et al., 2008). This procedure was designed to allow a fast throughput so that several litters can be examined daily within a relatively short period of time (Hill et al., 2008; Lim et al., 2008).

The day of birth was considered as postnatal day (PND) 0, in which pups were weighed and inspected for any gross malformations or particular traits. From that day on, mice were daily examined for the acquisition of developmental milestones and weight gain until PND 21, the weaning day. To allow for a fast identification of each mouse in a litter, on the first days after birth, pups were marked with a respective number and on PND 3, toe clipping was done not only for the identification of each mouse in the litter but also for proposes of genotyping.

On the day of testing, the home cage was moved into the testing room and left to habituate for at least 30 min. During the experimental execution, the pups were left in the same room as the mother and the time of separation was minimized as possible. The experimenter was always the same and identified the mouse by its marked number, being blind for the genotype. The execution of each test was random, as well as the animals order to perform them each day.

Each test has a range of time period during the 21 days to be performed (Table 3). The outcomes of the tests focus on the time to accurately perform, or respond to, a stimulus or posture.

Table 3: Data sheet for developmental milestones. Neonatal mouse pups were daily examined from PND 0 to 21 for performance on a battery of developmental tests assessing strength, coordination and the appearance of reflexes. The shaded areas identify the tests to be performed on each day.

Milestones test	Postnatal day																					
	0	1	2	3	4	5	6	7	8	9	10	11	12	13	14	15	16	17	18	19	20	21
Weight																						
Anogenital distance																						
Surface righting																						
Negative geotaxis																						
Cliff aversion																						
Rooting																						
Postural reflex																						
Wire suspension																						
Walking																						
Grasping																						
Auditory startle																						
Ear twitch																						
Open field																						
Air righting																						
Eye opening																						
Homing																						

Therefore, the latency of time (in seconds, s) for the animal to execute the test was registered and afterwards converted to dichotomic scores, as indicated in Table 4; this allows for a quantitative measurement of the behavior. The animal is considered to exhibit a mature response on a specific test when the highest score attributed is observed for two consecutive days (Hill et al., 2008; Lim et al., 2008).

Table 4: Conversion of time intervals registered for each test into dichotomic scores [adapted from (Hill et al., 2008)].

	Score			
	0	**1**	**2**	**3**
Surface righting	no response within 30 s	rights itself but slowly (10-25 s)	rights itself but it takes up to 10 s to do it	rights itself immediately in less than 1 s
Negative geotaxis	does not move at all within the 30 s period	turns its body 180º to the 'head up' position in a period time inferior to 30 s		
Cliff aversion	freezes/does not respond within the 30 s test-period	turns very slowly back to the surface (10-25 s)	avoids the cliff, but it still takes some time to turn, up to 10 s	turns back in less than 1 s
Rooting	does not move the head toward the filament	moves the head toward the filament		
Wire suspension	falls immediately	grasp the bar with all four limbs (maximum time set of 30 s)		
Auditory startle	does not jump	jump		
Ear twitch	not present	present		
Open field	does not respond in 30 s	moves out of the circle in less than 30 s		
Walking	no locomotion	*pivoting* – moving around with the help of the head and forelimbs, but not using the hind limbs	*crawling* – moving on all four limbs, dragging the belly over the surface	*walking* – mature locomotion with the body supported completely by the four limbs
Eye opening	both closed	one open	both open	
Air righting	lands on its back	lands on the surface with all four paws		
Grasping	no grasping	places its paw on the cotton bud, but it does not hold on firmly	places its paw on the cotton bud with more force, but when the cotton bud is pulled, cannot hold it	grasps the cotton bud very firmly
Postural reflex	not present	present		

Two independent groups of litters were used for the milestones evaluation. A first group of mating produced 5 litters each composed of between 5 to 12 pups, with a total of 35 pups (8 Wt, 16 Hetero and 11 LCN2-null offspring). All animals, both males and females, were submitted to the milestones protocol, and at the weaning day, they were housed in group of 5 animals in each cage and left to grow.

A second set of mating gave rise to 5 litters with a total of 42 pups (10 Wt, 20 Hetero and 12 LCN2-null). Again, all animals, males and females, were submitted to the milestones protocol but instead, at the PND 21, animals were sacrificed.

Each test and the time period of execution as well as the respective behavioral dimension that it evaluates, will be next described in detail (Hill et al., 2008; Lim et al., 2008) (summarized in Table 5).

Table 5: Summary of each test analyzed and the respective dimension that it evaluates.

	Somatic	Reflexes	Coordination	Strength	Vestibular	Olfactory
Weight	■					
Anogenital distance	■					
Eye opening	■					
Cliff aversion		■	■	■	■	
Negative geotaxis		■	■	■	■	
Surface/ Air righting		■	■	■	■	
Rooting		■	■			
Wire suspension				■		
Open field			■			
Walking			■			
Grasping		■				
Postural reflex		■				
Auditory startle		■				
Ear twitch		■				
Homing			■			■

Somatic parameters

As a measure for morphological development, animals were daily weighed and the anogenital distance (ANGD - distance between the opening of the anus and the opening of the genitalia) was measured. Eyes opening were also daily analyzed and a score was attributed as indicated in Table 4.

Neurological reflexes

Cliff aversion, PND1-14 (*Labyrinthine reflex and body righting mechanisms, strength, and coordination*)

In this test, the mouse pup was positioned on the edge of a small box with a smooth surface with the digits of the forepaws and the snout hanging over the edge of the box. The time for the pup to turn and begin to crawl away from the edge was registered. If the pup lost footing and slipped off the box, the test was repeated once more. If the mouse did not respond within 30 s, the test was terminated. The test was repeated daily until it was performed correctly in fewer than 30 s for two consecutive days.

Negative geotaxis, PND1–14 (*Labyrinthine reflex and body righting mechanisms, strength, and coordination*)

The animal was placed head down on a square of screen set at an angle of 45°. The time for the pup to turn 180° to the "head up" position was recorded. If the pup lost footing and slipped on the screen, the test was repeated once more. If the mouse did not respond within 30 s, the test was finished. The mature response was considered to be achieved when pups were able to perform correctly in fewer than 30 s for two consecutive days.

Surface righting, PND1-13 (*Labyrinthine reflex and body righting mechanisms, strength, and coordination*)

The mouse pup was held gently on its back and released. The time for the pup to flip over onto its abdomen with all four paws touching the surface of the table was registered. If the mouse did not respond within 30 s, the test was ended. The mature response was considered to be achieved when pups were able to right itself in less than 1 s for two consecutive days.

Air righting, PND8–21 (*Labyrinthine reflex and body righting mechanisms, strength, and coordination*)

The mouse pup held upside down was released from a height of approximately 60 cm and its landing position was examined. The first day that the pup landed right side up on all four paws was recorded. The test was repeated daily until the pup lands on all four paws for two consecutive days.

Rooting, PND1–12 (*Tactile reflex and motor coordination*)

A fine filament of cotton was used to perform this test. The filament was slowly and gently stroked three times from front to back along the side of the pup's head. Rooting occurred if the pup moved its head toward the filament. If there was no response to the brushing filament on one side of the head, the test was repeated once on the other side. Testing continued daily until the pup responded correctly for two consecutive days.

Wire suspension, PND4–14 (*Strength*)

The pup, hold with its forepaws in a 3-mm diameter metal wire suspended at 5 cm above a soft surface was released, and the length of time the mouse remains grasping the bar was measured. If the pup failed off immediately, the test was repeated once again. The test was repeated daily until the mature response was achieved when the animal was able to grasp the bar holding with all four limbs.

Open field, PND8–21 (*Locomotive coordination and extinguishing of pivoting behavior*)

In this test, a mouse pup is placed in the center of a circle with 13 cm in diameter and the time taken to move out was recorded. If the mouse did not respond in 30 s, the test was finished. The mouse was tested daily until it responded in fewer than 30 s for two consecutive days.

Walking, PND5-21 (*Locomotive coordination and muscular strength*)

In this test, the animals were able to freely move on the bench for 60 s. The first day the pups were able to move with the body completely supported by the four limbs was registered.

Grasping, PND5-21 (*Freeing reflex*)

The mouse pup palm forelimb was stimulated with a cotton swab. The day when the pup flexed the paw to grasp the object was recorded.

Postural reflex, PND5-21 (*Reflex*)

Animals placed in a small plastic box were gently shaken up and down and left and right. Acquisition of a mature postural reflex was considered when the animal was able to maintain its original position in the box by extending all four limbs.

Auditory startle, PND7–18 (*Auditory reflex*)

The mouse pup was placed on the laboratory bench, and its reaction to a handclap at a distance of 10 cm was recorded. The test was repeated daily until the pup responded correctly with a quick involuntary jump for two consecutive days.

Ear twitch, PND7–15 (*Tactile reflex*)

A fine filament twisted of a cotton swab was gently brushed against the tip of the ear three times. The pup was considered to achieve a mature response when it responded by flattening the ear against the side of the head for two consecutive days.

Homing, PND12 (*Locomotion and olfactory capabilities*)

Individual pups were placed in the center of a standard cage containing 1/3 of bedding from the home cage and the remaining 2/3 of the cage with new clean bedding. The latency to turn and move onto the home cage bedding was assessed in three separate trials. The pup was considered to have successfully 'homed' when all four paws had crossed onto the home cage bedding and the pup remained there for at least 10 s. Each trial lasted a maximum of 120 s with an inter-trial interval of approximately 10 s.

2.3.2 Adult behavior

Unraveling the role of LCN2 in the brain function included the use of a battery of standard tests that evaluate motor and locomotion, emotion (anxiety and depressive-like states) and cognition at adulthood. With that purpose, we submitted young adult (2-3 months old) LCN2-null male mice and their respective littermates to a set of behavioral paradigms (Figure 5).

Three independent set of animals from 3 different groups of matings, with a total of 28 Wt, 34 Hetero and 28 LCN2-null males animals were used. Not all sets were submitted to the same behavior tests, although some are common across them and when performed, the same timeline was used in the 3 independent experiences (Figure 5).

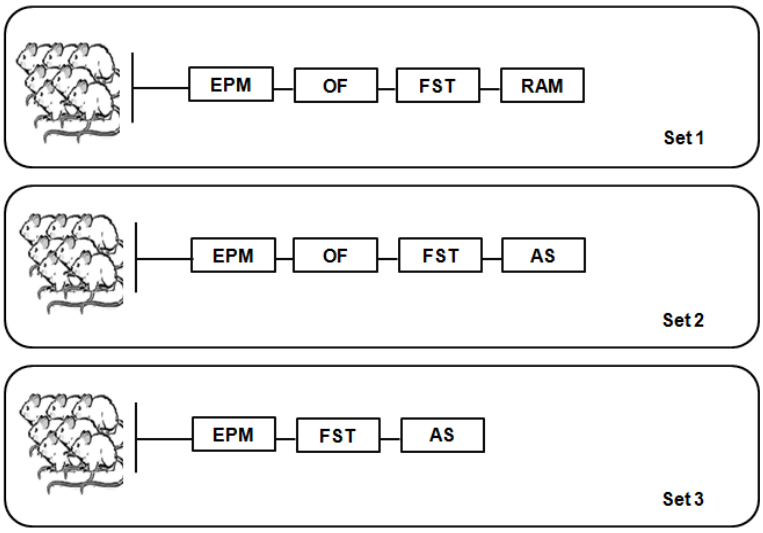

Figure 5: *Schematic representation of the timeline used for adult behavior*. For this assessment, 3 independent set of animals were used in 3 independent experiences. The order of tests presented corresponds to the order of performance done in each set. AS, Acoustic Startle; EPM, Elevated Plus Maze; FST; Forced Swim Test; OF, Open Field; RAM, Radial Arm Maze.

By the time of weaning, animals were housed 5 per cage and only handled in the week before the behavior protocol started in order to minimize the stress that could be caused by the experimenter manipulation. Tests were performed always in the light day period, since physiological and biochemical parameters change throughout the day (Wotjak, 2004). Before each test, animals were transferred to the test room for habituation for 30 min.

The detailed description of each test used will now be specified.

i) Elevated Plus Maze (EPM)

The EPM apparatus (ENV-560; MedAssociates Inc, St. Albans, VT, USA) was used to assess anxious-like behaviors and it consisted of two opposite open arms (50.8×10.2 cm) and two enclosed arms (50.8×10.2×40.6 cm) elevated 72.4 cm above the floor. The junction center area between the four arms measured 10×10 cm.

Mice were placed individually in the center of the maze facing a closed arm and were allowed to freely explore it for 5 min. Behavioral parameters were recorded with the use of an infra-red photobeam system connected to a computer with specific software (MedPCIV, MedAssociates Inc). The time spent in the closed arms was used to calculate the percentage of time in the closed arms which was taken as an index of anxiety-like behavior: the more time spent in the closed arms meant an anxious-like

state. The total number of entries in the closed arms was used as a measure of general locomotor activity.

ii) Open Field (OF)

The OF arena measures a combination of both exploratory and locomotor activities and aspects of anxiety. The OF apparatus consisted of a brightly illuminated square arena of 43.2×43.2 cm equipped with infrared beams located at the level of the arena floor on both X and Y axes (to monitor the central and peripheral horizontal activities) and above the floor on two sides of the chamber (to monitor vertical activity) (Med Associates Inc.). Mice were individually placed in the center of the arena and allowed to freely explore it for 5 min. The resulting data was analyzed using the Activity Monitor software (Med Associates, Inc.), considering two previously defined areas: a central and an outer area. Activity parameters such as total distance travelled, vertical activity and time spent in each predefined area, as well as the average velocity, were analyzed. Also, the ratio between the time spent in the center and in the periphery of the open field arena was used as an indicative of anxiety-like state (Prut and Belzung, 2003).

iii) Forced Swim Test (FST)

Learned helplessness was evaluated in the FST for the assessment of depressive-like behaviors. The test was conducted using a slightly modified method described by Porsolt and colleagues (1977) (Porsolt et al., 1977). Briefly, each animal was individually placed in glass cylinders filled with water (25°C; depth 30 cm) for 5 min. Test sessions were videotaped and manually scored as the immobility time and latency to immobility using the *Etholog V. 2.2* software, always by the same experimenter (Ottoni, 2000) blind to the animals genotype under assessment. The minimal duration for first bout of immobility was set at 1 s. A mouse was judged immobile when it ceased all active behaviors (i.e. struggling, swimming and jumping) and remained passively floating or making minimal movements necessary to maintain the nostrils above water (Castagne et al., 2009). Learned helplessness behavior was defined as an increase in time of immobility and a decrease in both latency to immobility and swimming time.

iv) Acoustic Startle (AS)

Startle reflexes to a sudden intense stimulus were assessed as a measured for the anxious-like state of the animal. For that, animals (2 animals in each trial) were placed in two independent startle response systems (SR-LAB™, San Diego Instruments, San Diego, CA, USA) each consisting of a non-restrictive Plexiglas cylinder (i.d. 8.9 cm, length 2.8 cm), mounted on a Plexiglas platform and placed in a ventilated, sound-attenuated chamber.

After a 5-min period of habituation, animals were subjected to serial startle stimulus, each one lasting 50 millisecond (ms), with a variety in intensity from 70 to 120 dB, in 10-dB increments. Stimuli were presented through a high frequency speaker located 33 cm above the startle chambers. Startle magnitudes were sampled each millisecond during a period of 200 ms beginning at the onset of the startle stimulus. Cylinder movements were detected and measured by a piezoelectric element mounted under each cylinder. The startle response was defined as the peak response during the 200 ms recording period and the higher the startle reflex, the more anxious is the state of the animal considered (Davis, 1990).

The test consisted of a two-day trial. The first day was used for the animals' habituation to the apparatus and light conditions presented for 5 min. The animals' response for the presence of the startle stimulus was only registered for the second day of test.

v) Cognitive Function Assessment

For cognitive evaluation purposes, two similar well described behavioral tests, the radial arm (RAM) and morris water mazes (MWM), were used. Of notice, each one was performed using two different mice strains, the BALB/c and C57BL/6, respectively, since the BALB/c strain is known to be a bad MWM performer (Yoshida et al., 2001). Also the respective littermates from each strain were used as controls.

Radial Arm Maze (RAM)

The RAM task has been most extensively used to investigate specific aspects of spatial working and reference memories. This task is based upon the premise that animals have evolved an optimal strategy to explore their environment and obtain food with the minimum amount of effort (Wenk, 2004).

The RAM apparatus was handmade with eight-radial arms each of them with 35 cm long and 5 cm wide, radiating from a 20 cm central platform at equal angles. Each arm

has a 5 mm-deep hole 1 cm from the end, which is used as a food cup. To eliminate possible bias caused by the smell of the pellet, the bottom of all the food cups at the end of the arms were baited. The apparatus was placed in a room where the conditions of light were low and visual distal cues were present in the walls (adapted from (Wenk, 2004)).

Briefly, approximately one week before the training session, animals (n_{Wt}=5, n_{Hetero}=5, $n_{LCN2\text{-}null}$=5) were food deprived until their body weight was reduced to 80–85% of the initial one. During this period, animals had access to food only for 1 h/day and were daily weighed to monitor health and degree of food deprivation. Throughout the acquisition period, animals were also food deprived, being only allowed to have access to food for 2 h after performing the test.

During the training period, which lasted 4 days, animals were individually placed on the maze for 10 min and allowed to freely explore it so they could get habituated to the apparatus. With the exception for the first day, in which no food was available in the apparatus, in the training period all the eight arms of the maze were baited with pellets (sweet cereals - Cheerios®). After these training trials, actual maze acquisition was performed on the following 6 days with one trial/day. At this point, only four of the eight arms were baited in a random alternate way always leaving an un-baited arm adjacent to each baited one. The food reward was placed at the end of each arm that had a visual distal cue associated. Animals were placed in the center of the maze and allowed to explore the maze completely and retrieve all food rewards. The trial was considered to be complete when all pellets were baited or until 10 min had elapsed, whichever occurred first.

All trials were videotaped and the number of entries into unbaited arms (reference memory errors) and re-entries in baited arms (working memory errors) were recorded, as well as the time elapsed between the beginning of the test session and the mice obtaining all available food rewards. Scores were manually attributed and counted using the *Etholog V. 2.2* software always by the same experimenter.

Morris Water Maze (MWM)

Cognition in the C57BL/6 mice (n_{Wt}=8, n_{Hetero}=8, $n_{LCN2\text{-}null}$=8) was conducted in a white circular tank (170 cm diameter) filled with water (23ºC; 31 cm of depth) placed in a poorly lit room with extrinsic clues. The water tank was divided in four imaginary quadrants and a platform (12 cm diameter; 30 cm high), invisible to the animals, was

placed in one of the quadrants. Trials were video-captured by a video-tracking system (Viewpoint, Champagne au mont d'or, France).

In this test, reference memory and reversal learning tasks were assessed, which are dependent on the cognitive function of the hippocampus and the PFC, respectively (Morris, 1984).

Reference Memory Task. In this task, which lasted 4 days, an escape platform was placed in one of the quadrants, and was maintained in the same position during the four daily trials. In each daily trial, animals were positioned in the water in a different starting point (north, east, west and south) facing the wall (to avoid habituation of the mouse to a particular area of the pool) and a trial was considered concluded when the platform was reached within the time-limit of 120 s. If the animals were unable to find the platform during the trial time, they were guided to the platform and allowed to stay in it for 30 s. The time required to reach the platform from the releasing point (latency escape time) and the distance swam (distance traveled by the animal from the releasing point to reach the platform, in cm) was recorded for the consecutive trials/days.

Reversal Learning Task. After conducting tests for 4 days with the platform in the same quadrant, in the 5^{th} and last day of the experiment the animals were tested for a reversal learning performance. Here, on the first trial out of four, the platform was removed and the animals were given a 60-s probe trial to test their memory, which was measured by the percentage of distance swum in the target quadrant (where the platform was during the acquisition phase of the test). Behavioral flexibility was evaluated in the 3 subsequent trials with a reverse task by positioning the platform in a new (opposite) quadrant from where it was placed during the acquisition phase of the protocol. This parameter was evaluated by the percentage of distances swum in both new and old quadrants.

2.4 Serum corticosterone measurements

Blood samples for basal measurements of corticosteroids were collected from animals of the Set 2 at the end of the experimental behavior assessment (Figure 5) (n_{Wt}=10, n_{Hetero}=8, $n_{LCN2\text{-}null}$=10). Collections were performed in two different time points, at both 8 a.m. and p.m., with an interval of 24 h in between. Serum was obtained by centrifugation (13.000 rpm for 10 min) and stored at -80ºC until further analysis. Subsequent serum corticosteroids levels were measured by radioimmunoassay

following the instructions provided by the manufacturer (MP Biomedicals, Inc., Orangeburg, NY, USA).

2.5 BrdU labeling *in vivo*

To assess the role of LCN2 on the proliferation at the neurogenic niches, young adult male LCN2-null mice and their respective littermates were intraperitoneally (i.p.) injected with a thymidine analogous that is incorporated in the DNA during the S-phase (Taupin, 2007), the bromodeoxyuridine (5-bromo-2'-deoxyuridine, BrdU) (50 mg/kg) and sacrificed 24 h later (n_{Wt}=5, n_{Hetero}=5, $n_{LCN2\text{-}null}$=8). To reduce stress-induced changes in the hypothalamic-pituitary-adrenal axis (HPA) axis associated with the injection, animals were daily handled for 1 week until the day of sacrifice.

At the sacrifice time, animals were anesthetized with ketamine hydrochloride (150 mg/Kg) plus medetomidine (0.3 mg/Kg), and transcardially perfused with cold saline (0.9% sodium chloride, NaCl) for the BrdU staining.

2.5.1 BrdU immunohistochemistry

At the sacrifice, brains were carefully removed, embedded in Tissue-Tek O.C.T. compound (Sakura Finetek Europe, Netherlands) and snap-frozen in liquid nitrogen.

Posterior serial coronal sections (20 μm) of the entire brain were cut in a cryostat and collected to slides for immunohistochemistry. Brain sections were fixed for 30 min with 4% paraformaldehyde (PFA), followed by a 10 min permeabilization step with 0.2% tris-buffer saline-tween (TBS-T). The antigen retrievel step was performed using the microwave oven as a heating device and the citrate buffer (pH 6.0) for 20 min. Following, the tissue acidification comprised incubation with 2M hydrochloric acid (HCl) for 30 min, after which sections were incubated for 10 min with 3% hydrogen peroxide (H_2O_2) for endogenous peroxidase blocking. Unspecific binding blockage was achieved by 30 min of incubation with 4% bovine serum albumin (BSA) (Sigma, St.Louis, MO, USA). The BrdU positive cells were labeled by overnight incubation with a primary antibody against BrdU at a dilution of 1:50 (Mouse Anti-Bromodeoxyurine, Clone Bu20a, DAKO, Barcelona, Spain). Detection was made using the Ultravision Detection System (Lab Vision, Freemont, CA, USA), and the reaction was developed with 3,3'-diaminobenzidine substrate (DAB; Sigma). At last, sections were counterstained with hematoxylin.

2.5.2 Stereology

The number of proliferating cells in the two neurogenic niches, namely the subependymal zone (SEZ) at the lateral ventricles and the subgranular zone (SGZ) of the dentate gyrus (DG) of the hippocampus, was estimated using the Visiopharm Integrator system (VIS) software (version 2.12.3.0) in an Olympus BX51 microscope (Olympus, Hamburg, Germany). Coronal sections for proliferation analysis comprised SEZ between bregma coordinates 0.86 mm and 0.14 mm, whereas SGZ was analyzed from -1.22 mm to -2.30 mm coordinates (Paxinos and Franklin, 2001).

Every sixteenth section from the anterior-posterior SEZ and SGZ was blindly analysed and the initial section to be analyzed was randomly selected to certify unbiased sampling. The number of BrdU positive cells in these areas was counted and results expressed as BrdU positive cells per area (in mm^2). The use of the VIS Software allowed delimitation, at low magnification (40x), of the areas of interest in the SEZ and SGZ and the counting of BrdU positive cells within the defined areas at high magnification (400x), in both the left and the right hemispheres.

In the particular case of the SEZ, data was obtained from specific regions in the anterior-posterior and dorsal-ventral axis taking in consideration SEZ topographical specificities, as described elsewhere (Falcão et al., 2012). Briefly, the SEZ was divided as anterior, intermediate and posterior, along the anterior-posterior axis, whereas along the dorsal-ventral axis the SEZ was defined as dorsal, ventral, dorsolateral and rostral migratory stream (RMS). All divisions are done based on differences in cell proliferation rates and intrinsic anatomy (Falcão et al., 2012). In addition to the analysis of proliferation within the SEZ areas, non-tangential proliferation from the SEZ was analyzed as the proliferation in the SEZ proximity, i.e., within 100-500 μm apart from the SEZ, along the anterior-posterior axis (Falcão et al., 2012).

With respect to the SGZ, the estimation of cell proliferation was performed as described by Silva and colleagues (2006). Briefly, within the DG different subdivisions, the SGZ was considered to be a 3-cell-body-wide zone at the border between the granular cell layer and the hilus (Silva et al., 2006).

2.6 Golgi staining

Adult brains (n_{Wt}=3, n_{Hetero}=3, $n_{LCN2\text{-}null}$=3) from mice that have been submitted to the behavioral analysis were transcardially perfused with saline under deep anesthesia as described before and processed for Golgi-Cox staining according to the protocol

described elsewhere (Gibb and Kolb, 1998). Briefly, at sacrifice, brains were removed and immersed in Golgi-Cox solution (a 1:1 solution of 5% potassium dichromate and 5% mercuric chloride diluted 4:10 with 5% potassium chromate (Glaser and Van der Loos, 1981) for 14 days; brains were then transferred to a 30% sucrose solution (minimum 3 days), before being cut on a vibratome. Coronal sections (200 μm) were collected in 6% sucrose and blotted dry onto cleaned, gelatin-coated microscope slides. They were subsequently alkalinized in 18.7% ammonia, developed in Dektol (Kodak, Linda-a-Velha, Portugal), fixed, dehydrated through a graded series of ethanols, cleared in xylene and mounted with entellan. Slides were coded before morphometric studies for blind analysis.

2.7 Dendritic tree analysis

Three-dimensional (3D) reconstructions of representative Golgi-impregnated neurons from the basolateral amygdala (BLA) and the bed nucleus of the stria terminalis (BNST) areas were assessed.

For the selection of the neuron to be reconstructed, the criteria described by Uylings (1986) and Radley (2004) was followed: i) full impregnation of the neurons along the entire length of the dentritic tree; ii) dendrites without truncated branches; iii) relative isolation from neighboring impregnated neurons to avoid interference with the analysis; and iv) no morphological changes attributable to incomplete dendritic impregnation of Golgi-Cox staining (Uylings et al., 1986; Radley et al., 2004).

In order to minimize selection bias, slices containing the region of interest were randomly searched and the first neurons fulfilling the criteria (maximum of 3 neurons per slice) were selected. For each selected neuron, all branches of the dendritic tree were reconstructed at 600x magnification using a motorized microscope (BX51, Olympus), with oil objectives, and attached to a camera (MicroBrightField Bioscience, Magdeburg, Germany) and with Neurolucida software (MicroBrightField Bioscience). 3D analysis of the reconstructed neurons was performed using NeuroExplorer software (MicroBrightField Bioscience).

In each brain, a total of 10 neurons were studied for each animal of the 3 genotype groups, and neurons from the same animal were averaged. Several aspects of dendritic morphology were examined. To assess overall changes, total dendritic length was compared between groups, as well as the percentage of spines on dendrites and the spine density (total spines divided by dendritic length). Sampling spine density was

designed as: i) dendritic branches were either parallel or at acute angles to the coronal surface of the section; ii) did not show overlap with other branches that would obscure visualization of spines; iii) were at a radial distance of the soma between 50 to 100 µm. For spine morphology assessment, spines in the selected segments were classified according to Harris and colleagues (1992) in mushroom, thin, tick, and ramified categories and the proportion of spines in each category was compared between groups (Harris et al., 1992).

To assess differences in the arrangement of dendritic material, a 3D version of a Sholl analysis (Sholl, 1956) was performed; for this, the number of intersections of dendrites with concentric spheres positioned at radial intervals of 20 µm from the soma was registered.

2.8 Statistical analysis

All statistical analysis was performed in GraphPad Prism 5.0 (GraphPad Software, Inc., La Jolla, CA, USA).

For multiple statistical comparisons between groups and with only one level of analysis, after confirmation of homogeneity, one-way ANOVA was used, with Bonferroni's multiple comparison test post hoc analysis. Data was considered as significant with $P \leq 0.05$ and as highly significant with $P \leq 0.001$. Whenever the homogeneity was not confirmed, the Kruskal-Wallis test, followed by Dunn's Multiple comparison test was performed. The same criteria for significance were applied in these situations. Two-way ANOVA repeated measures was used to analyze acoustic startle, cognitive tasks performance and Sholl analysis. Differences between groups were then determined by Bonferroni's multiple comparison test post hoc analysis. Statistical significance was accepted as previously. All data is presented as mean±SEM and as the average of all the experiments performed.

3.1 Impact of LCN2 in the normal brain development and function

3.1.1 Developmental milestones assessment

The results of the different behavioral parameters analyzed as the average of the two independent experiments we have performed are summarized and presented in Table 6 as the average of day of mature response within the 21 days of milestones protocol.
In general, no major gross and observable deficits were verified and all litters presented a normal development.

Somatic parameters

When evaluating the general body weight gain throughout the 21 days across genotypes, no differences were observed neither in males (F=0.58, P=0.98) or females (F=0.36, P=0.99) (Table 6). Relatively to the anogenital distance, also no differences were observed between genotypes (Table 6). Another hallmark for somatic development is the day of eye opening and for that we had constitutively registered the state of eyes opening until both eyes were found opened. All the animals independently of the genotype and gender have opened the eyes around PND 14 (males versus females: F=0.44, P=0.82).

Neurological reflexes

In the parameters examined to evaluate physical maturation of the newborn mice, all animals acquired almost at the same average day the mature response for each of the tests used (Table 6).
Regarding evaluation of reflexes and strength (air and surface righting), both males and females of all genotypes displayed the average day for the mature response around PND 10 (Table 6) (males versus females - air righting: F=1.56, P=0.17; surface righting: F=1.21, P=0.32). The same result was observed for the more specific tests used to assess reflexes, namely grasping, ear twitch and auditory startle, where animals, regardless of the gender, achieved maturation around PND 12 (Table 6) (grasping: F=1.22, P=0.31; ear twitch: F=0.29, P=0.92 auditory startle: F=0.96; P=0.45). With respect to the postural reflex, meaning the posture they present when gently shanked, no

impairments were found, with all animals exhibited such mature response already in the first days of performance, around PND 5 (data not shown).

The wire suspension test also allows for strength measurements and, as shown in Table 6, when comparing the three genotypes independently in both males and females, no differences in the mature acquisition were observed. When comparing the same parameter among the genotypes and considering both genders, again no distinction occurred, with animals acquiring a mature response around PND 15 (F=1.07, P=0.40).

As for the tests specifically used for motor coordination assessment, namely walking and open field, no differences across genotypes were observed, with an average of maturation day around PND 14 (Table 6). Inter-gender comparisons for both tests also suggests no differences (walking: F=0.22, P=0.95; open field: F=0.29, P=0.92)

Already at PND 12 it was possible to see that pups presented no locomotor impairments as seen in the homing test, a test that besides evaluating olfactory capabilities, it also requires locomotion. As data show (Table 6), no olfactory and motor deficits were presented in these animals, in both genders.

When analyzing the cliff aversion test, we found that LCN2-null mice had an average delay of 2.4 days for a mature acquisition when compared to the Wt offspring (mean of 3.66±0.72 versus 6.00±0.66; F=3.15, P<0.05). Interestingly, also the Hetero animals showed such delay (mean of 3.66±0.72 versus 6.07±0.76) (Figure 6A and in Table 6 - highlighted in grey). Of notice, this difference was only observed in males, as females in all the genotypes accomplished the test around the PND 3 (Figure 6A). It is evident that when inter-gender comparisons were made, LCN2-null males were in fact slower in the acquisition of a mature response when compared to the LCN2-null females (P<0.05) and the same occurred for the Hetero mice (F=6.89, P<0.05) (Figure 6A).

The cliff aversion test, together with the negative geotaxis, is particularly involved with the vestibular system development, meaning, the acquisition of spatial perception and coordination. Although not statistically significant, we observed that also in the negative geotaxis test the LCN2-null males present a slight delay of 1.13 days in the acquisition of the mature response, when compared to the Wt littermates (mean of 3.09±0.62 versus 4.22±0.36; P=0.23) (Table 6; Figure 6B). As for the females, no differences were noticed (F=0.22, P=0.80), as well as when inter-gender comparisons were made (F=0.50, P=0.77).

Table 6: Summary of the average days of mature response obtained in each genotype, both in males and females, during the developmental milestones assessment.

Milestones test	Males				
	Wt	Hetero	LCN2-null	*F*	*P-value*
Weight	5.75±0.547	6.07±0.58	5.79±0.54	0.58	0.99
Anogenital distance	6.46±0.54	6.81±0.57	6.70±0.56	0.23	1.00
Eye opening	14.25±0.32	13.79±0.28	14.00±0.36	0.57	0.57
Cliff aversion	3.66±0.72	6.07±0.76*	6.00±0.66*	3.15	0.05
Negative geotaxis	3.09±0.62	3.69±0.49	4.22±0.36	1.05	0.36
Air righting	10.67±0.55	9.26±0.33	9.70±0.49	2.64	0.09
Surface righting	10.67±0.44	9.27±0.46	9.57±0.42	2.66	0.09
Grasping	12.50±0.43	12.71±0.35	12.89±0.30	0.23	0.79
Rooting	3.60±0.40	4.80±0.58	3.75±0.62		0.27
Auditory startle	11.10±0.56	10.07±0.45	10.30±0.63	0.98	0.38
Ear twitch	12.90±0.37	12.42±0.49	12.50±0.37	0.35	0.71
Walking	14.08±0.41	13.57±0.41	13.89±0.61	0.34	0.71
Open field	14.09±1.11	13.91±0.85	13.25±1.16	0.16	0.85
Wire suspension	15.00±0.54	14.50±0.99	13.60±0.60	0.77	0.48
Homing	50.36±12.30	54.25±7.42	39.07±8.96	0.62	0.54

Milestones test	Females				
	Wt	Hetero	LCN2-null	*F*	*P-value*
Weight	5.41±0.51	6.06±0.59	6.00±0.57	0.36	0.99
Anogenital distance	4.48±0.38	4.65±0.34	4.80±0.32	0.31	1.00
Eye opening	14.00±0.25	13.82±0.16	13.85±0.22	0.13	0.88
Cliff aversion	2.50±0.42	2.54±0.45	2.67±0.60	0.03	0.98
Negative geotaxis	3.50±0.50	3.28±0.37	3.75±0.70	0.22	0.80
Air righting	10.50±0.42	10.19±0.34	10.23±0.62	0.08	0.93
Surface righting	9.60±0.50	8.94±0.41	9.00±0.56	0.27	0.76
Grasping	13.00±0.51	11.86±0.36	12.08±0.45	1.18	0.32
Rooting	5.0±1.73	3.75±0.64	6.00±1.03		0.27
Auditory startle	10.17±0.79	11.14±0.43	11.08±0.49	0.64	0.53
Ear twitch	12.00±2.00	12.36±0.30	12.30±0.44	0.06	0.94
Walking	13.50±0.76	13.73±0.35	13.54±0.43	0.08	0.92
Open field	14.50±1.17	14.76±0.66	14.56± 1.38	0.02	0.98
Wire suspension	14.33±0.66	14.33±0.58	15.71±0.28	1.70	0.21
Homing	50.39±16.88	64.05±7.38	57.51±9.93	0.39	0.68

*Significantly different when compared to Wt mice, $P<0.05$. Data is presented as the average day of mature activity acquired and represented as mean±SEM (Males: $n_{Wt}=9$, $n_{Hetero}=13$, $n_{LCN2\text{-}null}=9$; Females: $n_{Wt}=6$, $n_{Hetero}=11$, $n_{LCN2\text{-}null}=9$).

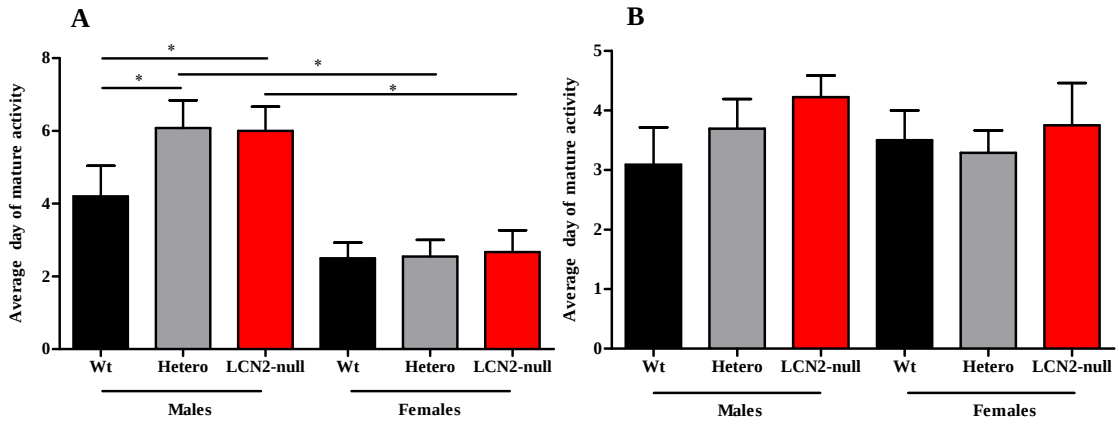

Figure 6: *Impact of LCN2 deletion in brain development and maturity*. Using a set of established tests used to evaluate neurologic parameters acquisition, from day 0 until PND21, LCN2-null mice were found to have a delay in the acquisition of a mature response on the cliff aversion (A) and the negative geotaxis (B) tests. These tests, performed from the PND 1 to 14, evaluate the acquisition of labyrinthine reflexes and body righting mechanisms, strength, and coordination, deeply associated to vestibular areas of the brain of spatial perception. Data are presented as the average day of mature activity. (Males: n_{Wt}=9, n_{Hetero}=13, $n_{LCN2\text{-}null}$=9; Females: n_{Wt}=6, n_{Hetero}=11, $n_{LCN2\text{-}null}$=9. Data presented as mean±SEM, **P*<0.05).

Altogether, no major impairments in relation to strength, motor/coordination and reflexes dimensions were observed in the LCN2-null animals, on both males and females. Even though, LCN2-null males, as well as the Heterozygous ones, display a delay in the acquisition of a mature response in the cliff aversion test, when compared to their Wt littermates. Interestingly, this delay was only visible in males, as females were much faster in the acquisition of the mature response. Of notice, this test is intrinsically associated to the vestibular system, brain areas of spatial perception and coordination.

3.1.2 Adult behavior performances

We started our behavior assessment by evaluating the anxious-like behavior of the LCN2-null animals through the EPM and AS tests and compared to both Wt and Hetero animals.

When analyzing the EPM data, LCN2-null animals clearly spent less time in the open arms (Wt=27.64±2.54, Hetero=26.29±2.95 and LCN2-null=13.88±2.45; F=6.96, P<0.001) (Figure 7A), which was reflected on the increased percentage of time spent in the closed arms (Wt=62.28±3.29, Hetero=62.94±3.64 and LCN2-null=74.48±2.86; F=3.71, P<0.05) (Figure 7B).

Importantly, the less time spent in each arm does not reflect less total activity in the apparatus by the LCN2-null animals, as the total number of entries in the closed arms

by these animals was similar when compared to their littermates (Wt=9.65±0.64, Hetero=8.08±0.77 and LCN2-null=7.90±1.03; F=1.44, P=0.25).

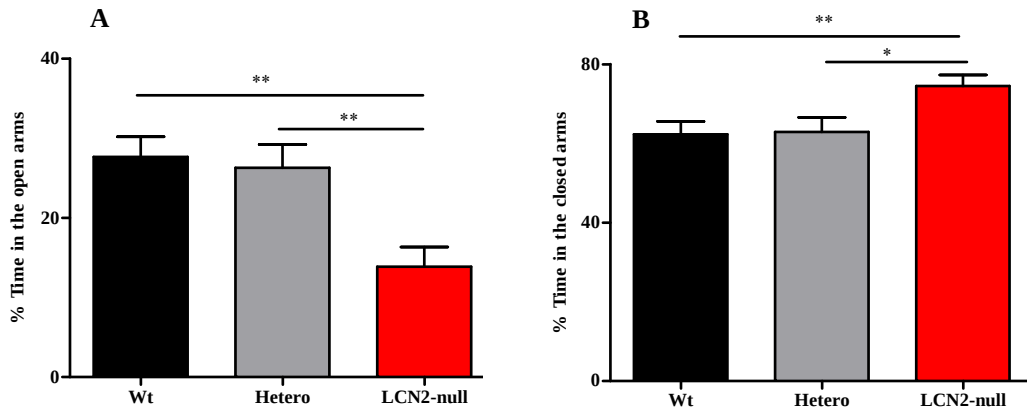

Figure 7: *Anxious-like behavior analysis in the elevated plus maze (EPM) test, as the percentage of time spent in each arm*. Decreased time spent in the open arms of the apparatus by the LCN2-null mice (A) and an increase in the time spent in the closed ones (B), reflect an anxious-like behavior of these animals. (n_{Wt}=23, n_{Hetero}=26, $n_{LCN2\text{-}null}$=19. Data presented as mean±SEM, *P<0.05, **P<0.001).

The following performance in the OF test allowed us to confirm the absence of major locomotor deficits, as analyzed by the total distance travelled by the animals in the open arena (Wt=3872±247.9, Hetero=3865±277.5 and LCN2-null=3652±252.0; F=0.24, P=0.79). Also, data concerning the exploratory activity of these animals (Wt=92.56±14.74, Hetero=87.67±12.29 and LCN2-null=86.68±11.76; F=0.06, P=0.94) and the average velocity displayed during the test (Wt=75.25±2.76, Hetero=80.01±3.13 and LCN2-null=75.52±3.49; F=0.70, P=0.49), evidenced for the absence of locomotive impairments.

Although it is not described as a classical test for anxiety, the OF can also be used as an indicator of possible anxious-like states of the animal, by the ratio of time spent in the center versus the periphery (Prut and Belzung, 2003). Data from the OF analysis regarding this ratio did not show differences in the time spent by the LCN2-null mice in the center of the arena versus the periphery (Wt=0.17±0.03, Hetero=0.14±0.02 and LCN2-null=0.16±0.03; F=0.42, P=0.66). Even though, data from EPM is more reliable as it is the classical-standard test for anxious-like behaviors measurements.

With respect to the AS test (Table 7), overall, all animals increased their startle response as the stimulus also increased, and although it seems that LCN2-null mice tend to

increase their response when compared to both controls, no significant differences were observed (F=0.99, P=0.45).

Table 7: Acoustic startle data represented as the startle amplitude response of the animals in the presence of increased acoustic stimulus (dB).

	Startle amplitude (arbitrary units)		
Stimulus (dB)	Wt	Hetero	LCN2-null
70	7.96±3.34	10.90±3.15	8.14±2.99
80	7.95±0.75	10.22±1.02	8.29±0.44
90	14.99±2.02	20.21±1.72	16.08±1.21
100	31.51±3.65	37.40±4.31	38.99±4.75
110	63.63±7.38	65.31±4.79	79.17±5.60
120	76.01±8.26	70.54±7.61	79.03±8.26

n_{Wt}=20, n_{Hetero}=21, $n_{LCN2\text{-}null}$=21. Data presented as mean±SEM

Taken together, it is clear that LCN2-null animals display an anxious-like phenotype, as measured by the EPM, suggesting a role for this protein in anxiety-related behaviors.

Following, and to assess depressive-like behaviors, we submitted the animals to the FST test to assay for their learned helplessness, indicative of a depressive-like behavior. Data from this test indicate that LCN2-null animals were significantly more prone to learned helplessness as observed by the increased immobility time (Wt=233.5±2.42, Hetero=244.0±2.30 and LCN2-null=249.2±1.78; F=11.97, P<0.0001) (Figure 8A) and the decrease in the latency time to an immobile posture (Wt=48.14±3.52, Hetero=47.84±2.49 and LCN2-null=37.40±2.81; F=4.11, P<0.05) (Figure 8B). Such increase in the time spent immobile was reflected by the decrease in the swimming time (Wt=66.56±2.42, Hetero=56.04±2.30 and LCN2-null=50.89±1.78; F=11.93, P<0.0001).

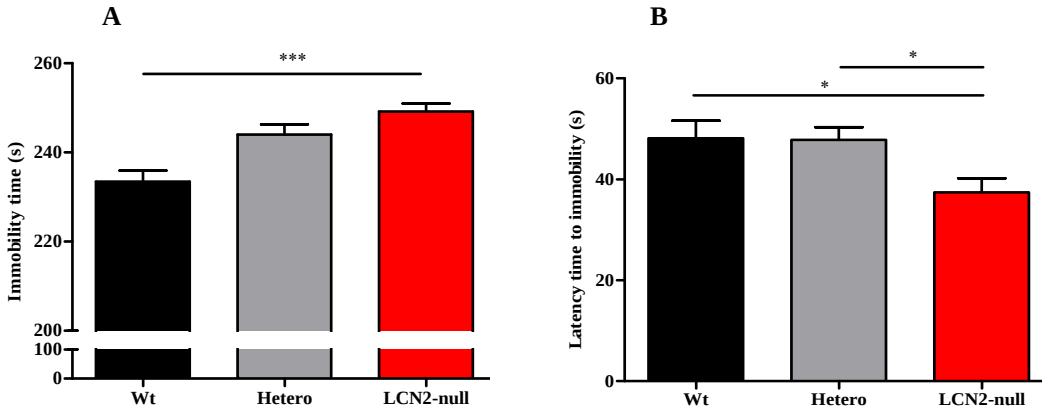

Figure 8: *Forced swim test (FST) for learned helplessness evaluation of LCN2-null mice and respective littermates*. Increased immobility time (A) for the LCN2-null mice and the decreased latency of time to acquire an immobile posture (B) are indicative of a depressive-like behavior for these animals. (n_{Wt}=30, n_{Hetero}=40, $n_{LCN2\text{-}null}$=33. Data presented as mean±SEM, **P*<0.05, ****P*<0.0001).

Overall, in addition for a role in anxiety-related behaviors, data from FST evidence further functions for LCN2 also in depression-like behaviors.

Since all the behavior tests performed and described so far were in the BALB/c background strain, we assessed cognition using the RAM, as it is described that this strain is not able to perform MWM tasks (Yoshida et al., 2001). Given that for the RAM test, long periods of fasting were required and because in the mean time we also had available in the lab a C57BL/6 strain with the same construct for LCN2 gene depletion, we submitted these animals to the MWM test to assess spatial and reference memories performances.

Regarding the RAM test, learning is indexed by the decrease in the latency of time to complete the test and by the decrease in the number of reference and working errors with the increased training. This task allows for the evaluation of both working (WM) and reference memories (RM). We observed that along the days, the decreased latency of time to complete the maze indicates that all animals have successfully explored the maze and readily consumed the pellets (Figure 9). No major differences were observed among the genotypes during the acquisition process (F= 0.48, P=0.89) (Figure 9).

The RM and WM components indicated that all animals made progressively fewer errors over the test-period and that no differences among the genotypes in learning processes was evident (RM: F=0.54, P=0.87; WM: F=0.27, P=0.99). Overall, data from

this test suggest for a successful process of learning among the genotypes and no major cognitive impairments.

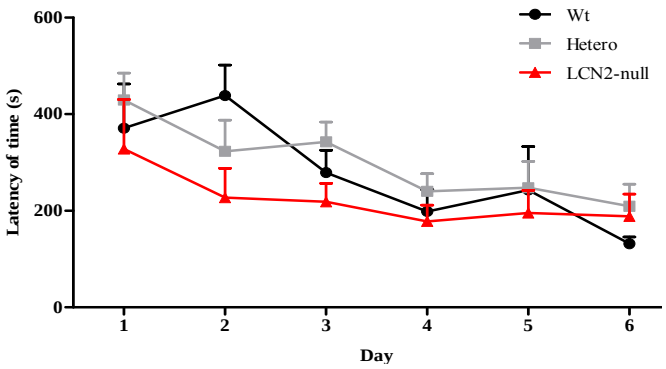

Figure 9: *Evaluation of spatial reference and working memory in the radial arm maze (RAM).* The latency of time to successfully complete the maze along the days is represented, and it is evident that no major cognitive and learning impairments were observed, as all the animals displayed a decrease of the time needed to complete the test over the days. (n_{Wt}=5, n_{Hetero}=10, $n_{LCN2\text{-}null}$=5. Data presented as mean±SEM).

Regarding the MWM in the C57BL/6 mice, we evaluated the latency of time to complete the task and the path length. During the acquisition phase it was clear that all animals have learned to find the hidden platform as shown by their improvement over the trials and along the days on the latency of time to complete the test (Figure 10). Even though it seemed that the LCN2-null mice required more time to complete the test along the days, which could reflect a worse performance in the task, but no statistical differences were seen (F=0.59, P=0.74) (Figure 10). Of notice, at the 4th day of the learning task, the time required to complete the test by both the LCN2-null and Hetero mice was even higher, but again no statistical significance was observed (F= 1.44, P=0.26). Concerning the path length travelled by the animals, this diminished throughout trials/days with no major differences between genotypes (F=0.67, P=0.67).

Interestingly, upon removal of the platform for the probe trial, and when evaluating the percentage of distance swum in each of the quadrants, all mice tested showed a high preference for the goal quadrant, i.e. where the platform was located during the acquisition phase (Wt=31%, Hetero=40% and LCN2-null=34%), but among them no major differences were found (F=1.21, P=0.31).

When behavioral flexibility was evaluated by changing the platform to the opposite quadrant, all animals behaved similarly in the sense that all still preferentially swum in the quadrant where the platform was at first. This was reflected by the less percentage of

distance swum in the new platform position (Old: Wt=34%, Hetero=35% and LCN2-null=33%; New: Wt=21%, Hetero=23% and LCN2-null=21%; $P<0.001$).

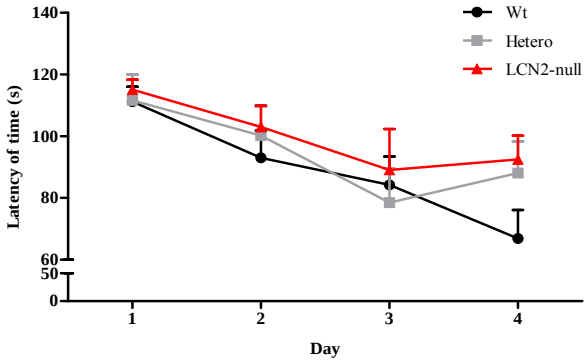

Figure 10: *Spatial reference memory in the Morris water maze (MWM) task*. Acquisition of the spatial reference memory task was comparable between groups based on the escape latency time. Along the days, it was evident that the learning process occurred similarly between all the animals, as they all decreased the latency of time to complete the task. ($n_{Wt}=8$, $n_{Hetero}=8$, $n_{LCN2\text{-}null}=8$. Data presented as mean±SEM).

In summary, no major cognitive impairments can be observed for these animals, as shown by the data from the RAM test for the BALB/c strain. A tendency for a worse performance, although not significant, was detected for the LCN2-null mice in the MWM.

3.2 Corticosteroid measurements

Adult behavior analysis of the LCN2-null mice and their littermates evidenced for a possible role for LCN2 in the modulation of emotion, namely in anxiety and depressive-like behaviors and this lead us to further verify the serum basal levels of corticosteroids. Blood collection occurred from animals of the Set 2 at the end of the behavioral analysis (Figure 5 – material and methods section).

The analysis of the corticosteroids levels revealed that animals did not show any alterations on both the morning and peak levels (morning: Wt=39.10±8.00, Hetero=76.88±23.95 and LCN2-null=39.19±8.82; $F=2.14$, $P=0.14$; peak: Wt=133.1±15.27, Hetero=183.6±31.51 and LCN2-null=128.2±24.59; $F=1.54$, $P=0.23$).

3.3 Morphological analysis of brain cytoarquitecture in LCN2-null mice

Having in mind the previous described phenotype for these mice, we performed neuronal morphology using Golgi impregnation techniques. Our first approach was to assess the brain regions described to be correlated with anxiety behaviors. Therefore, we

have started to analyze neurons from the basolateral amygdala (BLA) and bed nucleus of the stria terminalis (BNST) (Walker et al., 2003).

As presented in Table 8, we observed that in both BLA and BNST there were no significant differences among genotypes regarding the total dendritic length (BLA, *P*=0.33; BNST, *P*=0.88). Interestingly, data revealed that the absence of LCN2 led to an increase in spine density, although it did not reach statistical significance (Table 8). Of notice, such major differences only occurred in the BNST neurons (BLA, *P*=0.41; BNST, *P*=0.07) (Table 8-highlighted in grey; Figure 11).

Table 8: Influence of LCN2 in the morphometric analysis of dendrites of neurons of the BLA and BNST.

		Wt	Hetero	LCN2-null	*P-value*
BLA	Total dendritic length (µm)	1248±2.29	1214±166	1333±25.12	0.33
	Spine density (n/µm)	1.42±0.01	1.31±0.09	1.49±0.17	0.41
BNST	Total dendritic length (µm)	400.4±18.30	414.5±115.3	416.4±85.15	0.88
	Spine density (n/µm)	0.53±0.02	0.57±0.003	0.75±0.03	0.07

BLA, Basolateral amygdala; BNST, Bed Nucleus of Stria Terminalis. n_{Wt}=3, n_{Hetero}=3, $n_{LCN2\text{-}null}$=3; Data presented as mean ±SEM

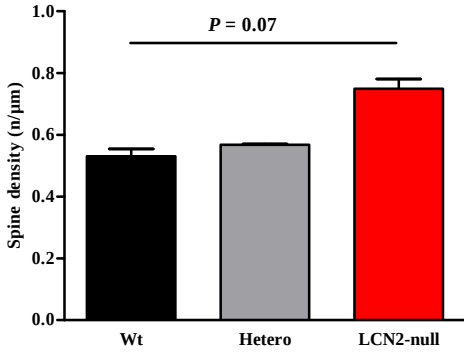

Figure 11: *Spine density assessment at the BNST neurons.* Analysis of the number of spines per dendritic length (n/µm) at the BNST has revealed that the absence of LCN2 lead to an increase in this parameter. (n_{Wt}=3, n_{Hetero}=3, $n_{LCN2\text{-}null}$=3. Data presented as mean±SEM).

We next examined the role of LCN2 in the regulation of spine morphology, by evaluating the proportion (as percentage) of each type of spines.

Such evaluation at the BLA region in the LCN2-null mice revealed no major differences irrespective of the type of spines, comparative to the littermate controls (Table 9). The proportion of each type of spines tended to be similar between animals (Figure 12A). Similarly, when analyzing the BNST region, we observed that the proportion of the different types of spines across genotypes revealed no major differences (Table 9, Figure 12B).

Table 9: Dendritic spines proportion assessment at the BLA and the BNST brain regions

		Wt	Hetero	LCN2-null	*P-value*
BLA	Mushroom	48.30±1.89	58.44±2.08	46.26±2.47	0.12
	Thin	27.03±2.83	29.85±3.97	29.59±2.66	0.39
	Thick	21.37±1.52	9.47±2.59	21.30±1.85	0.13
	Ramified	3.30±0.47	2.51±0.45	2.84±0.88	0.71
BNST	Mushroom	41.41±1.99	38.84±1.86	46.23±2.41	0.40
	Thin	43.22±0.70	44.77±0.11	38.67±5.13	0.41
	Thick	14.38±1.55	15.08±0.43	12.94±2.73	0.99
	Ramified	0.99±0.23	1.32±1.32	2.15±0.76	0.57

BLA, Basolateral amygdala; BNST, Bed Nucleus of Stria Terminalis. n_{Wt}=3, n_{Hetero}=3, $n_{LCN2\text{-}null}$=3; Data presented as mean ±SEM

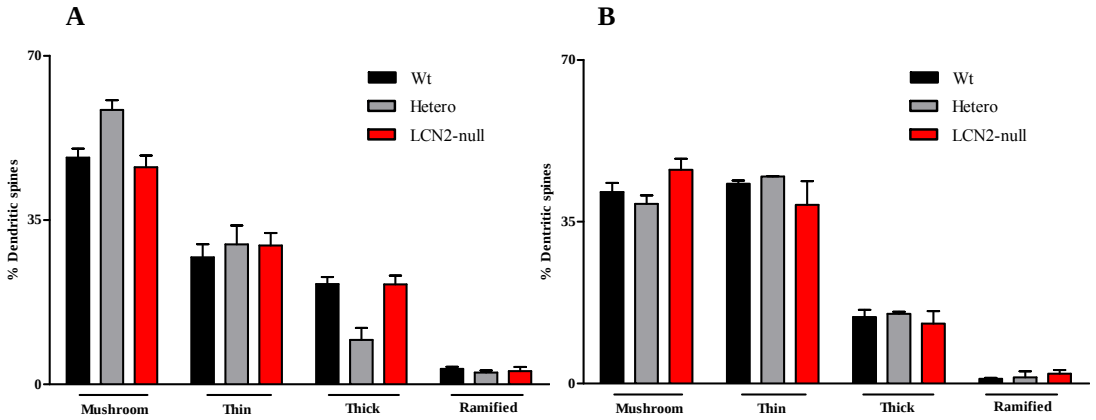

Figure 12: *Dendritic spines proportion of each type of spines analyzed at the BLA (A) and the BNST (B) brain regions.* When analyzing both BLA (A) and BNST (B) brain regions for the proportion of each spine, no differences were observed. (n_{Wt}=3, n_{Hetero}=3, $n_{LCN2\text{-}null}$=3. Data presented as mean±SEM).

Sholl analysis of the number of intersections as a function of their distance from the soma did not reveal any significant effects due to LCN2 absence on the BLA region (*F*=0.65, *P*=0.92; Figure 13A). As for the BNST, overall no differences in the 3D neuronal arrangement were observed in all the genotypes (*F*=1.05, *P*=0.35), but still LCN2-null mice seemed to present increased proximal ramification, as they presented a slight increase in the number of intersections at shorter distances (40 µm: Wt=4.22±0.17, Hetero=3.56±0.44 and LCN2-null=5.08±0.80) (Figures 13B,14).

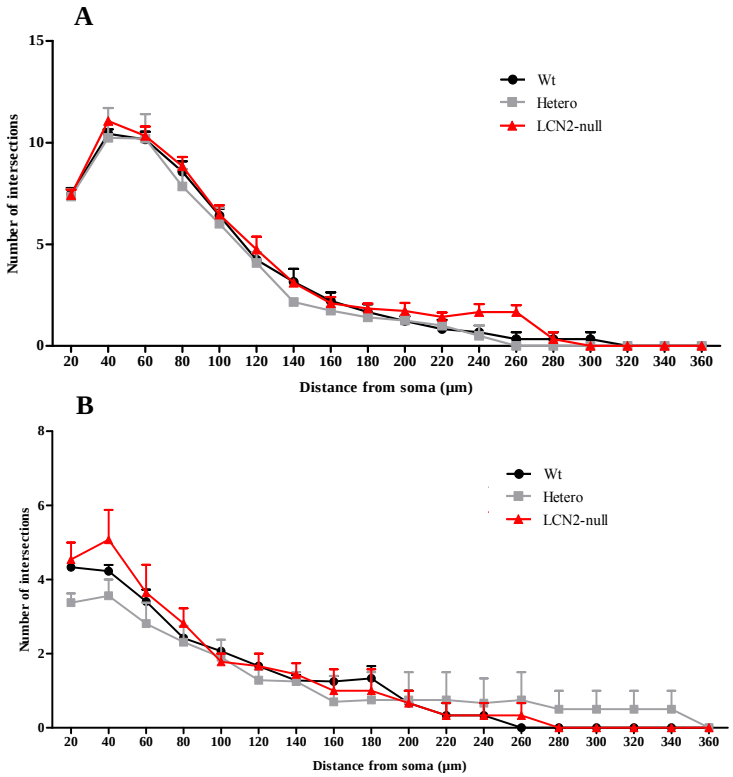

Figure 13: *Sholl analysis evaluation of the 3D reconstructed neurons, on both BLA (A) and BNST (B) brain regions*. No differences between genotypes were observed on both regions. Still, LCN2-null mice in the BNST seemed to present an increased proximal ramification (B). (n_{Wt}=3, n_{Hetero}=3, $n_{LCN2\text{-}null}$=3. Data presented as mean±SEM).

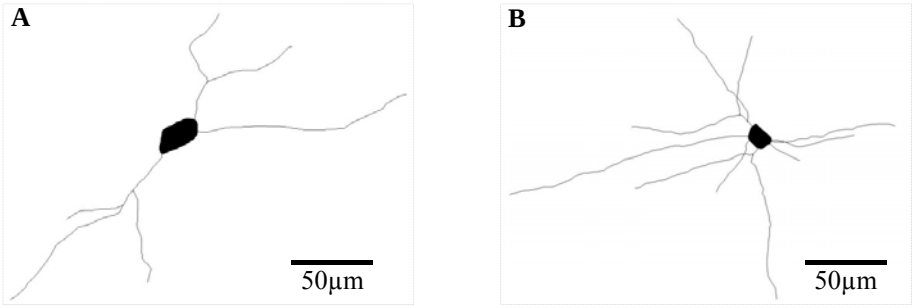

Figure 14: *3D reconstructions of BNST bipolar neurons of Wt (A) and LCN2-null (B) mice in the 3D spatial dimensions.* LCN2-null mice seemed to present increased proximal ramifications but the average dendritic length was similar between genotypes.

To summarize, in Table 10 a general overview of the major findings obtained for the brain morphological studies of the LCN2-null mice and their littermate controls is presented.

Table 10: Summary of all the results obtained for the morphological assessments in all the animals.

				Dendritic spines (%)				
		Dendritic length (µm)	Spine density (n/µm)	Mushroom	Thin	Thick	Ramified	Sholl analysis (number of intersections)
BLA	Wt	Similar	similar	similar				similar
	Hetero							
	LCN2-null[#]							
BNST	Wt	Similar	similar	similar				similar
	Hetero							
	LCN2-null[#]		increased					increased

[#] Compared to control littermates

3.4 Assessment of LCN2 impact on cell proliferation

Although the proliferation analysis at the SEZ included the analysis of the anterior-posterior axis and within each region the dorsal-ventral axis, as previously described in the material and methods section, for the purpose of this work we will only evaluate the results attending the dorsal-ventral axis at the intermediate level of the SEZ.

Results as the rates of proliferation (number of BrdU-positive cells per area) of the SEZ at the right hemisphere and taking into consideration the different divisions along the dorsal-ventral axis (ventral, dorsolateral, dorsal and RMS) showed no differences in the different regions (Table 11). When considering the total proliferation analysis as the average of the different previously mentioned divisions, again no differences between genotypes were found (Wt=3177±326.4, Hetero=3143±316.4 and LCN2-null=2893±194.3; P=0.67) (Figure 15A).

Table 11: Rates of proliferation in Wt, Hetero and LCN2-null mice, along the dorso-ventral axis at the intermediate level of the SEZ (considering the anterior-posterior axis). Data presented as the number of BrdU-positive cells per area of interest (mm^2).

	Wt	Hetero	LCN2-null	*P-value*
Ventral	3301±222.5	3151±236.4	2674±241.4	0.24
Dorsolateral	2547±476.0	2781±289.0	2962±259.0	0.31
Dorsal	1270±325.2	440±186.6	671±161.5	0.12
RMS	4381±282.1	3943±490.1	4230±483.4	0.71

RMS, Rostral Migratory Stream. n_{Wt}=5, n_{Hetero}=5, $n_{LCN2\text{-}null}$=8. Data presented as mean±SEM

In addition, the analysis of the non-tangential proliferation from the SEZ, i.e., within 100 and 500 µm apart from SEZ, along the anterior-posterior axis revealed that the number of cells proliferating was similar between genotypes (Wt=5.39±1.01, Hetero=5.08±0.67 and LCN2-null=4.63±0.69; *P*=0.87) (Figure 15B).

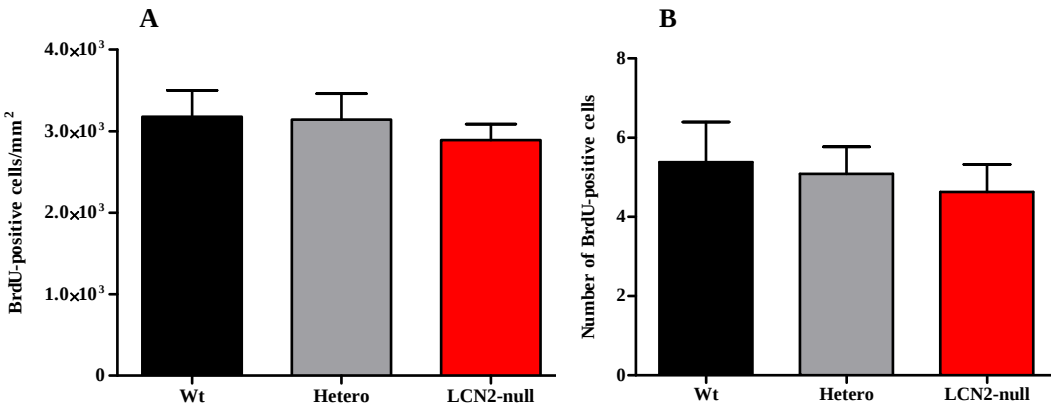

Figure 15: *Representative total proliferation at the intermediate level of the SEZ.* Total proliferation analysis, expressed as the number of BrdU-positive cells per area (mm^2), showed no differences among the genotypes (A). The number of proliferating cells at the vicinity of the SEZ at a distance of both 100 and 500 µm was also counted and found to also be similar among the genotypes (B). (n_{Wt}=5, n_{Hetero}=5, $n_{LCN2\text{-}null}$=8. Data presented as mean±SEM).

The same type of analysis was performed for the left hemisphere and the same patterns of proliferation were obtained in all animals, with no major differences to be considered (data not shown).

With respect to SGZ proliferation analysis, stereological analysis of the BrdU-positive cells within the 3-cell-body-wide zone in the DG and the respective cell proliferation estimation were done. Interestingly, no differences were found in the left hemisphere in

the different genotypes (Wt=308.2±75.11, Hetero=229.8±34.37 and LCN2-null=298.1±27.88; *P*=0.53). On the other hand, in the right hemisphere we found that the number of BrdU-positive cells was significant decreased in the LCN2-null mice, comparative to both Wt and Hetero animals (Wt=270.1±29.56, Hetero=273.4±19.38 and LCN2-null=202.6±16.32; *P*<0.05) (Figure 16).

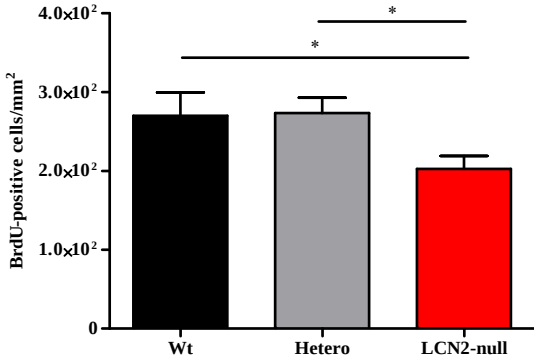

Figure 16: *Representative total proliferation at the SGZ of the DG*. Assessment of the total proliferation occurring at the SGZ of Wt, Hetero and LCN2-null animals show that LCN2-null mice had less proliferation, as indicated by the decreased number of BrdU-positive cells per area (mm^2). (n_{Wt}=5, n_{Hetero}=5, $n_{LCN2\text{-}null}$=8. Data presented as mean±SEM, **P*<0.05).

Therefore, additional roles for LCN2 are brought into light, this time by its possible function in the modulation of cell proliferation.

To summarize, all the parameters analyzed when comparing the LCN2-null mice with its respective Wt and Hetero animals are presented in Table 12.

Table 12: Summary of the data obtained during this project regarding the role of LCN2 in the CNS.

			Wt	Hetero	LCN2-null*
Neurodevelopmental	Milestones	Cliff aversion	-	delayed#	delayed
		Negative geotaxis	-	delayed#	delayed
Adult behavior	Anxiety	EPM	-	-	increased
		Acoustic Startle	similar		
	Locomotion	OF	similar		
	Depression	FST	-	-	increased
	Cognition	RAM	similar		
		MWM (C57BL/6 strain)	similar		
Morphology	Golgi studies	BLA	See Table 10 (page 56)		
		BNST			
Cell proliferation	BrdU-labelling	SEZ	similar		
		SGZ	-	-	decreased

EPM, Elevated Plus Maze; OF, Open Field; FST, Forced Swim Test; RAM, Radial Arm Maze; MWM, Morris Water Maze; BLA, Basolateral Amygdala; BNST, Bed Nucleus of the Stria Terminalis; SEZ, Subependymal Zone; SGZ, Subgranular Zone

* Compared to control littermates

Compared to Wt animals

CHAPTER 4 - DISCUSSION

The work developed and presented here was designed to analyze the physiological role of LCN2 in the CNS and its contribution in several aspects of brain function. Using an animal model with a targeted deletion of *Lcn2* gene we were able to ascertain some of the contributions of this protein in many brain processes, from the development until adulthood, and also at the morphological and cellular levels.

Overall, we were able to show the putative involvement of LCN2 in brain development and maturation processes and its contributions in triggering both hyperanxiety (measured by EPM) and depressive-like behaviors (assessed by FST) in adulthood. At the level of the brain morphometrics, changes in the spine density at the BNST neurons were observed for the LCN2-null mice as well as an increased dendritic proximal ramification. Additional studies on the impact of LCN2 on the cellular level have revealed a role for this protein in the modulation of the hippocampus SGZ cellular proliferation.

Altogether, the data presented herein provides new insights on the physiological role of LCN2 in the CNS, not much explored so far, contributing to a better understanding of its broad attributed functions.

4.1 LCN2 during brain development

At least in peripheral organs, LCN2 has been shown to be involved in the first stages of cell/tissue development and differentiation, not only in embryonic phases but also as shortly after birth through its capacity to bind and transport iron into or from the cells. A classical example is the kidney, where LCN2 was shown to regulate epithelial morphogenesis, being iron an important issue in this process (Yang et al., 2002).

To assess the impact of LCN2 on neurodevelopment, we used the milestones protocol, a simple procedure that is easy to measure, require little equipment and included a battery of assays as indicator of both neurological, strength and motor development (Hill et al., 2008).

In general, all litters that have been tested for the milestones protocol presented a normal development and no particular traits were noticed in the timing of eye opening,

body weight and anogenital distance, which are mainly physical and somatic, nor in the specific motor development as assessed by the open field and walking tests, or in the sensorial parameters, as evaluated by grasping, auditory startle, rooting and ear twitch.

The only differences found were on the cliff aversion and negative geotaxis tests, as seen by the delay in the timing (measured as days) to acquire a mature response in the LCN2-null males: a delay of almost 3 days for the cliff aversion and of 1 day in the negative geotaxis were observed. This was gender specific, since LCN2-null females had a similar maturation as the littermate Wt and Hetero animals. These observations are of interest given the reported gender differences in neuronal maturation (Mesquita et al., 2007). Interestingly, also the male Hetero animals presented such delay, suggesting that even the presence of one copy of the gene is not sufficient to oppose the delayed effects of LCN2 absence in males' brain maturation.

Associated with the vestibular areas of the brain, the cliff aversion and negative geotaxis behaviors require the maturation of underlying labyrinthine and body righting mechanisms in this area, and such described delays suggest that developing may occur at slower rates in the LCN2-null mice when compared to Wt controls. Interestingly, other tests such as postural and righting reflexes (air and surface) also depend on the development of dynamic postural adjustments but that in addition implies the integrity of muscular and motor function, that were not altered. This may be due to underlying neural circuits in these tests that differ from the ones of cliff aversion and negative geotaxis, thus revealing these differences.

In rodents, cliff aversion and negative geotaxis behaviors are describe to develop soon after birth and the timing of their appearance and development has been suggested as a parameter for the assessment of the overall development of the rodent nervous system (Hill et al., 2008). These reflexes are sensitive to the function of the vestibular system, of which the role is to provide information on the position and movement of body and head in space - the sense of spatial orientation (Altman and Sudarshan, 1975). It is largely dependent on brainstem structures that act as a central processor, exchanging signals for movement and body position through some pathways to several other brain regions (e.g. cerebellum and spinal cord) (Altman and Sudarshan, 1975).

It is, therefore, interesting to notice that the absence of LCN2 induces a delay in the maturation of the brainstem, curiously one of the brain regions that have already been described to highly express LCN2 in basal conditions in adulthood (Chia et al., 2011).

It is also possible that during development, LCN2 has a differential expression pattern, which deserves further investigation and may provide additional clues regarding its mechanism of action. The precise mechanisms underlying the observed impairment are still to be clarified, but it may be related to the role of LCN2 in iron delivery to cells, which influences proliferation and maturation, as suggested. In fact, iron is required for neurodevelopment namely for cell division, neurotransmitters synthesis and myelinization (Lozoff and Georgieff, 2006). The vestibular system is known to receive serotonergic enervations (Mesquita et al., 2007) and monoamines (norepinephrine and serotonin) and their metabolites have been found to be present at endogenous levels in vestibular nucleus (Cransac et al., 1996). In this context, iron deficiency affects regional monoamine metabolism, in part likely due to iron-dependent enzymes; in fact, several studies have shown that early iron deficiency is associated with alterations within dopaminergic systems (Lozoff and Georgieff, 2006; Unger et al., 2007). The distribution of monoamines, in particular dopamine, and iron in the brain are closely related and indeed monoaminergic transmition is very sensitive to perturbations in iron delivery (Lozoff and Georgieff, 2006). As an iron-transporter protein known to modulate several cellular processes, we can speculate that the iron levels in the LCN2-null mice could be lower comparatively with those in Wt controls and in this way this could contribute to possible dysfunction in the vestibular system maturation. It is however difficult to justify or speculate why other areas of the brain did not show similar impairment. Further understanding of the underlying mechanisms can be obtained by measurement of the neurotransmitter levels in various brain regions, which should be done next.

It is however clear that the absence of LCN2 does not impair the overall normal neuronal development. Probably, even if a major contribution by LCN2 occurs for certain brain systems maturation and development, similar to what occurs in the periphery, its effects are somehow compensated. Similarly, despite the descriptions of its involvement in kidney cell development, animals with deletion of LCN2 are viable and present normal kidney functions (Flo et al., 2004; Berger et al., 2006). Therefore, a high redundancy of LCN2 role in development, despite the context, seems to exist.

4.2 The adult brain function and the contribution of LCN2

Interestingly, it has been described that adult phenotypes and brain functions can be influenced by possible deficits in one or more functional domains during

neurodevelopment (Van der Meer et al., 2001). In fact, several studies have raised the possibility that neurodevelopmental abnormalities specifically in the brain stem act in concert to contribute to psychopathologies later in life (Mesquita et al., 2007).

Whether this is or not correlated to the previous described delays in development, we found that in the adult brain, LCN2 is involved in triggering emotional behaviors, namely anxious and depressive-like behaviors.

Based on the neurodevelopment observations, we chose the male to further study behavior in adulthood. The focus on males also reduces the heterogeneity usually associated with female behavior analysis due to the female hormonal status.

Male LCN2-null mice displayed both a hyperanxiety state, as demonstrated by the increased percentage of time spent in the closed arms of the EPM apparatus, and a depressive-like behavior, translated in the increased learned helplessness in the FST. Importantly, we found no differences in motor performances, which are of relevance since many of the behavior tests used require locomotor activity evaluation; we can therefore exclude motor impairment as a possible confounding effect of the behavioral assessment. Therefore, these observations indicate that genetic disruption of LCN2 facilitates the development of anxiety and depression behaviors.

Of interest, a recent study reports no differences in anxiety in basal conditions in LCN2-null mice, but rather that this disruption of the *Lcn2* gene promoted stress-induced increase in spine density and caused an increase in the proportion of mushroom spines. The above changes correlated with higher excitability of CA1 principal neurons and with elevated stress-induced anxiety in LCN2-null mice. In this study, the authors showed that LCN2 promotes stress-induced changes in spine morphology and function to regulate neuronal excitability and anxiety (Mucha et al., 2011).

For the assessment of learning and memory tasks, we started with the evaluation of BALB/c mice in the RAM test, since this strain is described to perform poorly in the more conventional MWM test (Chapillon and Debouzie, 2000; Yoshida et al., 2001).

While we found no differences between the genotypes, this evaluation was difficult to perform given the requirement for long periods of food deprivation that was too aggressive for the animals, which made us to not repeat this experimental protocol. In the meantime, LCN2-null mice in the C57BL/6 background became available, allowing us to study cognitive performances using the MWM, since mice from this strain are claimed to be good performers (Vorhees and Williams, 2006).

In this test, animals are motivated by the desire to escape to a safe platform that is precisely located and with the help of external visual spatial clues the animal can learn its position. Results regarding the latency of time along the days to complete the task did not reveal any major impairment for the LCN2-null mice, even though a slight tendency to an increased latency of time compared to control was observed, mostly seen at the 4th day, where the LCN2-null animals tend to became worse in their performances. Of relevance, such tendency was not a result of a slower swimming rate, as we have not found differences in this parameter (data not shown). Still, no major conclusions can be assumed from this test since on the reversal evaluation on the 5th day all the animals still had a higher preference for the quadrant of the 'old' position of the platform, suggesting that animals, independently of the genotype, have not successfully learned the aim of the test. Since we have only performed this test once, we plan next to increase the time period of acquisition from 4 to 5 days, and the performance of 2 days for the reverse task (Vorhees and Williams, 2006).

4.3 The hypothalamic-pituitary-adrenal (HPA) axis in LCN2-null mice

The HPA axis is the major neuroendocrine system that controls organism reactions. As a response to stress, the axis releases corticotrophin-releasing hormone (CRH) from the paraventricular nucleus of the hypothalamus, which in turn acts on the pituitary gland stimulating the release of adrenocorticotropin (ACTH) into the circulation. In the periphery, glucocorticoids (corticosteroids in rodents) are then secreted from the adrenal gland. A negative feedback mediated by glucocorticoids on the hypothalamus, pituitary and higher brain centers ensures the equilibrium of the system (Femenia et al., 2012). Most importantly, the HPA axis is also responsible for the regulation of many body processes including mood and emotions (Femenia et al., 2012). Therefore, as we observed an altered basal emotional state in our LCN2-null mice, we hypothesized that alterations within the HPA axis of the animals could be mediating such phenotype.

In this context, we have assessed the corticosteroid levels of LCN2-null mice in comparison with their littermate controls. In all genotypes, corticosterone levels were measured at both 8 a.m. and at 8 p.m. given the well described circadian rhythm of the hormone (Romero, 2002). Independently of the period of the day in which blood was collected, no differences among genotypes were observed.

Of interest, Mucha and colleagues (2011) showed evidence for a role for LCN2 in response to stress, when submitting LCN2-null mice to a physiological restrain as a

stress paradigm (Mucha et al., 2011). However, they do not mention or presented data concerning the corticosteroids levels in these animals, neither in basal or in stress conditions (Mucha et al., 2011). For that reason, it will be of interest also to check the corticosteroid levels of these animals when submitted to stress, as the response to this condition may differ from that observed in basal states.

Altogether, and since no differences were found in the corticosteroid levels of our animals, the HPA axis is not likely to be the reason for the altered anxious and depressive-like behaviors observed in the LCN2-null mice.

4.4 Uncovering the role of LCN2 in neuronal morphology and its implications in emotional behaviors

Adjustments in spine density, morphology, and neuronal excitability may result in alterations of the behavioral phenotype. Hereupon, our next step was to analyzed LCN2-null mice brain morphometrics, more precisely neuronal morphology by means of Golgi impregnation. We chose to firstly study the BLA within the amygdala and the BNST, given the well recognized link with emotional behaviors (Walker et al., 2003; Pego et al., 2006; LeDoux, 2007).

No changes were found in dendritic length, arborization and spine density and morphology in the amygdala, but the 3D reconstruction of BNST bipolar neurons revealed that LCN2-null mice displayed a trend to increased proximal ramification, as verified by the Sholl analysis, but with no changes in the overall dentritic length. In addition, the absence of LCN2 led to an increased spine density, with no major differences in spine morphology between genotypes.

Vyas and colleagues (2003) have shown that in anxious-like states, triggered by chronic stress in animals, the amygdala neuronal dendritic arborization remains unaffected but an increased arborization in BNST neurons was observed (Vyas et al., 2003). As our LCN2-null mice are ‘naturally’ anxious, the tendency for an increased proximal ramification suggests the involvement of LCN2 in dendritic remodeling of BNST neurons thus triggering anxiety-like behaviors. Moreover, Pêgo and colleagues (2008) have shown the occurrence of increased spine density at the BNST in anxious animal models, although triggered by stress, but with no volumetric or morphological changes in the amygdala (Pego et al., 2008).

Interestingly, Mucha and colleagues (2011) have also showed that in basal states, LCN2-null mice present an increased spine density at the CA1-CA3 hippocampus, also

with no alterations in spine morphology (Mucha et al., 2011). This result led the authors to suggest an additional role for LCN2 in spine destabilization and elimination (Mucha et al., 2011). In accordance, our data analysis of BNST neurons further suggests the possible role for LCN2 in spine elimination in emotional-related brain regions.

The changes in dendritic arborization and the higher spine density in the BNST neurons observed in LCN2-null mice may have important physiological consequences. Dendritic spines morphology and function are dynamic and modulated by input-specific neuronal activities. Changes in their morphology are known to affect synaptic and local circuit organizations, and stable neuronal circuits are achieved by a balance in declined spine elimination and increased spines half-life (Alvarez and Sabatini, 2007). Inevitably, alteration in this balance will ultimately lead to altered emotional responses (Alvarez and Sabatini, 2007; von Bohlen Und Halbach, 2009). The presented increased spine density in our LCN2-null mice can ultimately be correlated and translated with the altered emotional behaviors observed. The mechanism underlying such changes in spines is not clear. An insight on the involvement of actin is advanced by Mucha and colleagues (2011) that suggested that LCN2 is involved in actin dynamics and mobility (Mucha et al., 2011). Complementary, in their work they have exposed hippocampal cultured neurons to both holo and apo-LCN2, and a prominent decrease in spine density was seen when cells were exposed to holo-LCN2, further enhanced when apo-LCN2 was added, consolidating the idea for LCN2' function in spine elimination (Mucha et al., 2011).

More importantly, iron seems to be a crucial factor in the modulation of such functions by LCN2. At least in the hippocampus, it has been shown that in cases of iron depletion there is a reduced hippocampal dendritic arborization that can lead to impaired behaviors (Jorgenson et al., 2003).

Until now, the precise pathways through which LCN2 is involved in the alteration of the BNST are not clear. Still, we can hypothesize that the absence of LCN2, and therefore hypothetical decreased iron levels, can ultimately impair normal dendritic modulation. This, in turn, culminates with altered emotional behaviors.

Depression and anxiety share considerable comorbidity, and probably the features found at the level of the morphology in the BNST can explain the referred alterations on both dimensions in the LCN2-null mice. Additionally, some authors have shown that in both depressed patients and animals models there is a dendritic atrophy and reduced spine

density in the hippocampus (von Bohlen Und Halbach, 2009; Femenia et al., 2012). Therefore, our morphometric studies should be extended to other affective-related brain areas, such as the hippocampus.

Also of relevance would be the evaluation of LCN2 levels in animal models of depression and anxiety.

4.5 LCN2 modulation of cell proliferation at the neurogenic niches

The following evaluation of the proliferative profiles of adult neural stem cells in the LCN2-null animals was motivated by two main reasons: first due to the described linkage of emotional behaviors with alterations in cell proliferation and second because, at least in the periphery, LCN2 has been shown to be involved in cell proliferation.

In the adult brain, neural stem cells are restricted to specific well-defined regions that allow for a permissive microenvironment for their proliferation and maintenance (Kazanis, 2009; Ming and Song, 2011). Neurogenesis, as it is called the process by which neural stem cells proliferate, differentiate and give raise to new functional neurons, occurs at the SGZ of the hippocampal DG and the SEZ of the lateral ventricles (Kazanis, 2009; Ming and Song, 2011). Importantly, this is a dynamic process, intrinsically modulated by several molecular and physiological factors (Ming and Song, 2011).

The precise contribution of LCN2 in the modulation of neural stem cells proliferation has not been reported so far, but several evidences show its involvement in cellular apoptosis and proliferation (Yang et al., 2002; Devireddy et al., 2005).

Stereological analysis of the total number of BrdU-positive cells per area on both niches revealed that the absence of LCN2 does not influence proliferation in the SEZ, but does lead to a decreased cell proliferation in the SGZ.

Of notice, we identified that the decreased cellular proliferation only occurs in the right hemisphere of the LCN2-null mice, whereas on the left side the rates were similar between genotypes. This regional difference is in accordance with other reports that show SGZ neurogenesis to occur differentially in the hemispheres (Silva et al., 2006). A possible role for LCN2 in the hippocampus is interesting, since Chia and colleagues (2011) showed that the hippocampus was the brain region that presented the lowest LCN2 basal levels of expression, at least in the adult rat brain (Chia et al., 2011), but its

expression is up-regulated in response to stress (Mucha et al., 2011) and after kainate treatment (Chia et al., 2011).

Interestingly, this observation in the decrease in the SGZ cellular proliferation may be related with the observed behavioral phenotype in LCN2-null mice, since the hippocampus is a crucial structure for emotion processing (Femenia et al., 2012). A prevailing assumption in the field of adult neurogenesis is that the continuous generation of new neurons within the hippocampus offers, in addition to synaptic plasticity, a cellular flexibility to the system. A bulk of studies support the concept that young neurons contribute and facilitate the execution of hippocampal-dependent tasks like learning and memory (dorsal hippocampus), but also in emotional responses (ventral hippocampus) (Vaidya et al., 2007; Couillard-Despres et al., 2011). In fact, reduction or blockage of neurogenesis is not only associated with cognitive impairments (Couillard-Despres et al., 2011), but also emotional states, including mood and anxiety-like behaviors (Bessa et al., 2009).

It is noteworthy to point out that the hippocampus cytoarchitecture results from the balance between the integration of new neurons (neurogenesis) and the concurrent elimination of neurons through apoptosis (Couillard-Despres et al., 2011). Remarkably, this physiological equilibrium has ultimate implications in mood (Silva et al., 2006; Couillard-Despres et al., 2011). The dual role displayed by LCN2 on both processes should be further explored in this context. We should next study how apoptosis is affected in LCN2-null mice, particularly since Bim expression, a pro-apoptotic factor, has been implied in the LCN2 cascade triggering apoptosis (Devireddy et al., 2005).

Finally, it would also be of interest to characterize which brain cells are being affected by these deficits in proliferation.

CHAPTER 5 – CONCLUDING REMARKS

Lipocalin-2 is a protein that has been gain a great deal of interest in multidisciplinary fields over the last two decades since its discovery. Initially, due to its notable broad expression and rapidly induction upon stimulus and in tissues more prone to infection, the relevance of LCN2 in defense strategies mechanisms was denoted. As part of the innate immune response, LCN2 is able to bind iron-loaded siderophores secreted by bacteria during infection and thus limit their growth. Just recently, the described capacity of LCN2 to interact with specific cell surface receptors (24p3R) and the evidence for the existence of an endogenous mammalian siderophore has brought into light its significance in mediating cellular processes through iron, even in physiological states. In fact, it is believed that is through the iron binding capacity that LCN2 is broadly accepted to engage roles ranging from cell proliferation and survival, tissue development and protection, up to apoptosis. At least in the kidney, LCN2 is known to modulate organ development soon after birth but also to confer tissue protection upon injury. However, at the same time, LCN2 functions do not seem to be detrimental, as animals with a targeted deletion of LCN2 appear healthy and show normal kidney development being their major feature the increased susceptibility to bacterial infections.

The studies addressing LCN2 involvement in cellular processes are in part limited to the periphery being its role in the CNS context less explored. Most of the reports demonstrate LCN2 as an important molecule in the diseased brain, namely during multiple sclerosis, Alzheimer and in response to injury being the astrocytes, and also in some cases neurons, the brain cells responsible for the production of the protein *in vivo*. In addition, its behavior as an acute-phase protein at the barriers of the brain, namely the endothelial cells of the blood brain barrier and the epithelial cells of the CP, adds its involvement in the mechanisms of brain immune defense. Interestingly, LCN2 is also known to be up-regulated by glucocorticoids, being also described as having a critical role as mediator of the stress response at the subcellular, morphological, and behavioral levels.

In what concerns the physiological brain, some questions remain unexplored: does LCN2 have a function? Does it employ the same cellular strategies as extensively described in the periphery, through iron? Although low levels of LCN2 are occurring in

the healthy brain, the description of both the 24p3R and protein expressions on specific regions, allied with its iron-trafficking properties, gives insights onto possible roles also in the physiological brain.
Therefore, we sought to investigate how LCN2 could impact on the physiological brain, in an attempt to fill the gap that exist and likely to uncover new possible roles.

Behavioral analysis of the LCN2-null mice firstly soon after birth gave us some insights on the possible involvement of LCN2 in specific brain regions development and maturation. As data from the cliff aversion reveals, LCN2-null males mice presented a substantial delay in acquiring a mature response in the test, which may indicate delays in the maturity of vestibular brain regions related with visual spatial acquisition and perception. Later in adulthood, LCN2 was observed to trigger altered emotional states, as LCN2-null mice displayed both hyperanxious and depressive-like behaviors. In addition, morphological and cellular approaches evidenced the contribution of LCN2 in the BNST spine density regulation and in hippocampal cell proliferation, which can ultimately culminate in the altered described behaviors. Respectively, LCN2-null mice were shown to present increased spine density in the BNST, with no major alterations in the amygdala, which in turn can explain the hyperanxious state presented by these animals. As for the hippocampal cell proliferation, LCN2-null mice presented decreased cell proliferation and survival, which evidenced for the possible involvement of LCN2 in the modulation of cell proliferation that in turn can culminate with the altered behaviors.
Altogether, LCN2 involvement on both cell proliferation modulation and neuronal plasticity can account for the altered emotional states that the LCN2-null mice present. In fact, it is possible that these two phenomena are intimately connected, where LCN2 assumes a major role.

Although we were able to give some insight onto the role played by LCN2 in the brain, still much further work is required as our findings have brought many additional questions than the ones we had when we first started this project.
Indeed, how is LCN2 modulating brain development and why this engagement in such specific brain regions? Are the levels of neurotransmitters altered during development? The role of amygdala in triggering emotional states in our animals was set aside, but is the BNST the only emotional-related area involved? Is in fact the role of LCN2 in spine

elimination and stabilization the only contributor to those altered behavioral states? And how is iron involved or even if it is involved at all? Proliferative profiles of adult neural stem cells seem to explain, in part, the engaged depressive-like behaviors by the LCN2-null mice. But how is LCN2 modulating hippocampal cell proliferation? And which types of cells are bearing from its absence that can ultimately lead to depression and anxiety states?

These and many other underlying questions are the ones we hope to, in a near future, answer and likely add new lights on LCN2 role in the physiological brain function.

CHAPTER 6 – REFERENCES

Allen, R., Erickson, R., and Jesaitis, A. (1989). Identification of a human neutrophil protein of *Mr* 24 000 that binds *N*-formyl peptides: co-sedimentation with specific granules. *Biochim Biophys Acta* 99**,** 123-133.

Altman, J., and Sudarshan, K. (1975). Postnatal development of locomotion in the laboratory rat. *Anim Behav* 23**,** 896-920.

Alvarez, V.A., and Sabatini, B.L. (2007). Anatomical and physiological plasticity of dendritic spines. *Annu Rev Neurosci* 30**,** 79-97.

Anderson, G.J., and Frazer, D.M. (2005). Hepatic iron metabolism. *Semin Liver Dis* 25**,** 420-432.

Bao, G., Clifton, M., Hoette, T.M., Mori, K., Deng, S.X., Qiu, A., Viltard, M., Williams, D., Paragas, N., Leete, T., Kulkarni, R., Li, X., Lee, B., Kalandadze, A., Ratner, A.J., Pizarro, J.C., Schmidt-Ott, K.M., Landry, D.W., Raymond, K.N., Strong, R.K., and Barasch, J. (2010). Iron traffics in circulation bound to a siderocalin (Ngal)-catechol complex. *Nat Chem Biol* 6**,** 602-609.

Berard, J.L., Zarruk, J.G., Arbour, N., Prat, A., Yong, V.W., Jacques, F.H., Akira, S., and David, S. (2012). Lipocalin 2 is a novel immune mediator of experimental autoimmune encephalomyelitis pathogenesis and is modulated in multiple sclerosis. *Glia* 60**,** 1145-1159.

Berger, T., Togawa, A., Duncan, G.S., Elia, A.J., You-Ten, A., Wakeham, A., Fong, H.E., Cheung, C.C., and Mak, T.W. (2006). Lipocalin 2-deficient mice exhibit increased sensitivity to Escherichia coli infection but not to ischemia-reperfusion injury. *Proc Natl Acad Sci U S A* 103**,** 1834-1839.

Bessa, J.M., Ferreira, D., Melo, I., Marques, F., Cerqueira, J.J., Palha, J.A., Almeida, O.F., and Sousa, N. (2009). The mood-improving actions of antidepressants do not depend on neurogenesis but are associated with neuronal remodeling. *Mol Psychiatry* 14**,** 764-773.

Bolignano, D., Donato, V., Lacquaniti, A., Fazio, M.R., Bono, C., Coppolino, G., and Buemi, M. (2010). Neutrophil gelatinase-associated lipocalin (NGAL) in human neoplasias: a new protein enters the scene. *Cancer Lett* 288**,** 10-16.

Borregaard, N., Sehested, M., Nielsen, B., H., S., and Kjeldsen, L. (1995). Biosynthesis of granule proteins in normal human bone marrow cells. Gelatinase is a marker of terminal neutrophil differentiation *Blood* 85**,** 812-817.

Castagne, V., Moser, P., and Porsolt, R.D. (2009). "Behavioral assessment of antidepressant activity in rodents," in *Methods of Behavior Analysis in Neuroscience. 2nd edition.*, ed. J.J. Buccafusco. 2011/01/05 ed (Boca Raton (FL): CRC Press).

Chakraborty, S., Kaur, S., Guha, S., and Batra, S. (2012). The multifaceted roles of neutrophil gelatinase associated lipocalin (NGAL) in inflammation and cancer. *Biochim Biophys Acta* 1826**,** 129-169.

Chan, Y.R., Liu, J.S., Pociask, D.A., Zheng, M., Mietzner, T.A., Berger, T., Mak, T.W., Clifton, M.C., Strong, R.K., Ray, P., and Kolls, J.K. (2009). Lipocalin 2 is required for pulmonary host defense against Klebsiella infection. *J Immunol* 182**,** 4947-4956.

Chapillon, P., and Debouzie, A. (2000). BALB/c mice are not so bad in the Morris water maze. *Behav Brain Res* 117**,** 115-118.

Chia, W.J., Dawe, G.S., and Ong, W.Y. (2011). Expression and localization of the iron-siderophore binding protein lipocalin 2 in the normal rat brain and after kainate-induced excitotoxicity. *Neurochem Int* 59**,** 591-599.

Choi, J., Lee, H.W., and Suk, K. (2011). Increased plasma levels of lipocalin 2 in mild cognitive impairment. *J Neurol Sci* 305**,** 28-33.

Coles, M., Diercks, T., Muehlenweg, B., Bartsch, S., Zoèlzer, V., Tschesche, H., and Kessler, H. (1999). The Solution Structure and Dynamics of Human Neutrophil Gelatinase-associated Lipocalin. *J. Mol. Biol.* 289**,** 139-157.

Couillard-Despres, S., Iglseder, B., and Aigner, L. (2011). Neurogenesis, cellular plasticity and cognition: the impact of stem cells in the adult and aging brain-a mini-review. *Gerontology* 57**,** 559-564.

Cowland, J., Muta, T., and Borregaard, N. (2003). IL-1beta-specific up-regulation of neutrophil gelatinase-associated lipocalin is controlled by IkappaB-zeta. *J Immunol* 176**,** 5559-5566.

Cowland, J.B., and Borregaard, N. (1997). Molecular characterization and pattern of tissue expression of the gene for neutrophil gelatinase-associated lipocalin from humans. *Genomics* 45**,** 17-23.

Cransac, H., Cottet-Emard, J.M., Pequignot, J.M., and Peyrin, L. (1996). Monoamines (norepinephrine, dopamine, serotonin) in the rat medial vestibular nucleus: endogenous levels and turnover. *J Neural Transm* 103**,** 391-401.

Davis, M. (1990). Animal models of anxiety based on classical conditioning: the conditioned emotional response (CER) and the fear-potentiated startle effect. *Pharmacol Ther* 47**,** 147-165.

De Biase, A., Knoblach, S.M., Di Giovanni, S., Fan, C., Molon, A., Hoffman, E.P., and Faden, A.I. (2005). Gene expression profiling of experimental traumatic spinal cord injury as a function of distance from impact site and injury severity. *Physiol Genomics* 22**,** 368-381.

Devireddy, L., Teodoro, J., Richard, F., and Green, M. (2001). Induction of apoptosis by a secreted lipocalin that is transcriptionally regulated by IL-3 deprivation. *Science* 293**,** 829-834.

Devireddy, L.R., Gazin, C., Zhu, X., and Green, M.R. (2005). A cell-surface receptor for lipocalin 24p3 selectively mediates apoptosis and iron uptake. *Cell* 123**,** 1293-1305.

Devireddy, L.R., Hart, D.O., Goetz, D.H., and Green, M.R. (2010). A mammalian siderophore synthesized by an enzyme with a bacterial homolog involved in enterobactin production. *Cell* 141**,** 1006-1017.

Falcão, A.M., Palha, J.A., Ferreira, A.C., Marques, F., Sousa, N., and Sousa, J.C. (2012). Topographical analysis of the subependymal zone neurogenic niche. *PLoS One* 7**,** e38647.

Femenia, T., Gomez-Galan, M., Lindskog, M., and Magara, S. (2012). Dysfunctional hippocampal activity affects emotion and cognition in mood disorders. *Brain Res*.

Flo, T.H., Smith, K.D., Sato, S., Rodriguez, D.J., Holmes, M.A., Strong, R.K., Akira, S., and Aderem, A. (2004). Lipocalin 2 mediates an innate immune response to bacterial infection by sequestrating iron. *Nature* 432**,** 917-921.

Flower, D.R. (1994). The lipocalin protein family: a role in cell regulation. *FEBS Lett* 354**,** 7-11.

Flower, D.R. (1996). The lipocalin protein family: structure and function. *Biochem J* 318 1-14.

Flower, D.R., North, A.C.T., and Sansom, C.E. (2000). The lipocalin protein family: structural and sequence overview. *Biochim Biophys Acta* 1482**,** 9-24.

Friedl, A., Stoesz, S., Buckley, P., and Gould, M. (1999). Neutrophil gelatinase-associated lipocalin in normal and neoplastic human tissues. Cell type-specific pattern of expression. *Histochem J* 31**,** 433-441.

Garay-Rojas, E., Harper, M., Hraba-Renevey, S., and Kress, M. (1996). An apparent autocrine mechanism amplifies the dexamethasone- and retinoic acid-induced expression of mouse lipocalin-encoding gene 24p3. *Gene* 170**,** 173-180.

Garrick, M.D., and Garrick, L.M. (2009). Cellular iron transport. *Biochim Biophys Acta* 1790**,** 309–325.

Gibb, R., and Kolb, B. (1998). A method for vibratome sectioning of Golgi-Cox stained whole rat brain. *J Neurosci Methods* 79**,** 1-4.

Glaser, E.M., and Van Der Loos, H. (1981). Analysis of thick brain sections by obverse-reverse computer microscopy: application of a new, high clarity Golgi-Nissl stain. *J Neurosci Methods* 4**,** 117-125.

Goetz, D., Holmes, M., Borregaard, N., Bluhm, M.E., Raymond, K.N., and Strong, R.K. (2002). The neutrophil lipocalin NGAL is a bacteriostatic agent that interferes with siderophore-mediated iron acquisition. *Mol Cell* 10**,** 1033-1043.

Goetz, D., Willie, S., Armen, R., Bratt, T., Borregaard, N., and Strong, R. (2000). Ligand Preference Inferred from the Structure of Neutrophil Gelatinase Associated Lipocalin. *Biochemistry* 39**,** 1935-1941.

Gomme, P.T., Mccann, K.B., and Bertolini, J. (2005). Transferrin: structure, function and potential therapeutic actions. *Drug Discov Today* 10**,** 267-273.

Grzyb, J., Latowski, D., and Strzaika, K. (2006). Lipocalins - a family portrait. *J Plant Physiol* 163**,** 895-915.

Guo, H., Jin, D., Zhang, Y., Wright, W., Bazuine, M., Brockman, D.A., Bernlohr, D.A., and Chen, X. (2010). Lipocalin-2 deficiency impairs thermogenesis and potentiates diet-induced insulin resistance in mice. *Diabetes* 59**,** 1376-1385.

Gwira, J.A., Wei, F., Ishibe, S., Ueland, J.M., Barasch, J., and Cantley, L.G. (2005). Expression of neutrophil gelatinase-associated lipocalin regulates epithelial morphogenesis in vitro. *J Biol Chem* 280**,** 7875-7882.

Harris, K., Jensen, F., and Tsao, B. (1992). Three-dimensional structure of dendritic spines and synapses in rat hippocampus (CA1) at postnatal day 15 and adult ages: implications for the maturation of synaptic physiology and long-term potentiation. *J Neurosci* 12**,** 2685-2705.

Harrison, P.M., and Arosio, P. (1996). The ferritins: molecular properties, iron storage function and cellular regulation. *Biochim Biophys Acta* 1275**,** 161-203.

Hentze, M.W., Muckenthaler, M.U., and Andrews, N.C. (2004). Balancing acts: molecular control of mammalian iron metabolism. *Cell* 117**,** 285-297.

Hill, J.M., Lim, M.A., and Stone, M.M. (2008). "Developmental milestones in the newborn mouse," in *Neuropeptide Techniques,* ed. I. Gozes. (Tel Aviv: Humana Press), 131-149.

Holmes, M., Paulsene, W., Jide, X., Ratledge, C., and Strong, R. (2005). Siderocalin (Lcn 2) also binds carboxymycobactins, potentially defending against mycobacterial infections through iron sequestration. *Structure* 13**,** 29-41.

Hraba-Renevey, S., Turler, H., Kress, M., Salomon, C., and Weil, R. (1989). SV40-induced expression of mouse gene 24p3 involves a post-transcriptional mechanism. *Oncogene* 4**,** 601-608.

Hvidberg, V., Jacobsen, C., Strong, R.K., Cowland, J.B., Moestrup, S.K., and Borregaard, N. (2005). The endocytic receptor megalin binds the iron transporting neutrophil-gelatinase-associated lipocalin with high affinity and mediates its cellular uptake. *FEBS Lett* 579**,** 773-777.

Ip, J.P., Nocon, A.L., Hofer, M.J., Lim, S.L., Muller, M., and Campbell, I.L. (2011). Lipocalin 2 in the central nervous system host response to systemic lipopolysaccharide administration. *J Neuroinflammation* 8**,** 124.

Jin, D., Zhang, Y., and Chen, X. (2011). Lipocalin 2 deficiency inhibits cell proliferation, autophagy, and mitochondrial biogenesis in mouse embryonic cells. *Mol Cell Biochem* 351**,** 165-172.

Jorgenson, L.A., Wobken, J.D., and Georgieff, M.K. (2003). Perinatal iron deficiency alters apical dendritic growth in hippocampal CA1 pyramidal neurons. *Dev Neurosci* 25**,** 412-420.

Jun, L.S., Siddall, C.P., and Rosen, E.D. (2011). A minor role for lipocalin 2 in high-fat diet-induced glucose intolerance. *Am J Physiol Endocrinol Metab* 301**,** E825-835.

Karlsen, J.R., Borregaard, N., and Cowland, J.B. (2010). Induction of neutrophil gelatinase-associated lipocalin expression by co-stimulation with interleukin-17 and tumor necrosis factor-α is controlled by IκB-ζ but neither by C/EBP-β nor C/EBP-δ. *J Biol Chem* 285**,** 14088-14100.

Kazanis, I. (2009). The subependymal zone neurogenic niche: a beating heart in the centre of the brain: how plastic is adult neurogenesis? Opportunities for therapy and questions to be addressed. *Brain* 132**,** 2909-2921.

Kehrer, J.P. (2010). Lipocalin-2: pro- or anti-apoptotic? *Cell Biol Toxicol* 26**,** 83-89.

Kjeldsen, L., Bainton, D.F., Sengelsv, H., and Borregaard, N. (1994). Identification of neutrophil gelatinase-associated lipocalin as a novel matrix protein of specific granules in human neutrophils *Blood* 83**,** 799-807.

Kjeldsen, L., Cowland, J.B., and Borregaard, N. (2000). Human neutrophil gelatinase-associated lipocalin and homologous proteins in rat and mouse. *Biochim Biophys Acta* 1482**,** 272-283.

Kjeldsen, L., Johnsen, A.H., Sengelov, H., and Borregaard, N. (1993). Isolation and primary structure of NGAL, a novel protein associated with human neutrophil gelatinase. *J Biol Chem* 268**,** 10425-10432.

Krause, A., Neitz, S., Magert, H.J., Schulz, A., Forssmann, W.G., Schulz-Knappe, P., and Adermann, K. (2000). LEAP-1, a novel highly disulfide-bonded human peptide, exhibits antimicrobial activity. *FEBS Lett* 480**,** 147-150.

Lafon-Cazal, M., Adjali, O., Galeotti, N., Poncet, J., Jouin, P., Homburger, V., Bockaert, J., and Marin, P. (2003). Proteomic analysis of astrocytic secretion in the mouse. Comparison with the cerebrospinal fluid proteome. *J Biol Chem* 278**,** 24438-24448.

Law, I.K., Xu, A., Lam, K.S., Berger, T., Mak, T.W., Vanhoutte, P.M., Liu, J.T., Sweeney, G., Zhou, M., Yang, B., and Wang, Y. (2010). Lipocalin-2 deficiency attenuates insulin resistance associated with aging and obesity. *Diabetes* 59**,** 872-882.

Ledoux, J. (2007). The amygdala. *Curr Biol* 17**,** R868-874.

Lee, S., Kim, J.H., Seo, J.W., Han, H.S., Lee, W.H., Mori, K., Nakao, K., Barasch, J., and Suk, K. (2011). Lipocalin-2 is a chemokine inducer in the central nervous system: role of chemokine ligand 10 (CXCL10) in lipocalin-2 induced cell migration *J Biol Chem* 286**,** 43855-43870.

Lee, S., Lee, J., Kim, S., Park, J.Y., Lee, W.H., Mori, K., Kim, S.H., Kim, I.K., and Suk, K. (2007). A dual role of lipocalin 2 in the apoptosis and deramification of activated microglia. *J Immunol* 179**,** 3231-3241.

Lee, S., Lee, W.H., Lee, M.S., Mori, K., and Suk, K. (2012). Regulation by lipocalin-2 of neuronal cell death, migration, and morphology. *J Neurosci Res* 90**,** 540-550.

Lee, S., Park, J.Y., Lee, W.H., Kim, H., Park, H.C., Mori, K., and Suk, K. (2009). Lipocalin-2 is an autocrine mediator of reactive astrocytosis. *J Neurosci* 29**,** 234-249.

Li, C., and Chan, Y.R. (2011). Lipocalin 2 regulation and its complex role in inflammation and cancer. *Cytokine* 56**,** 435-441.

Lim, M.A., Stack, C.M., Cuasay, K., Stone, M.M., Mcfarlane, H.G., Waschek, J.A., and Hill, J.M. (2008). Regardless of genotype, offspring of VIP-deficient female mice exhibit developmental delays and deficits in social behavior. *Int J Dev Neurosci* 26**,** 423-434.

Liu, Q., and Nilsen-Hamilton, M. (1995). Identification of a New Acute Phase Protein. *J Biol Chem* 270**,** 22565–22257.

Liu, Z., Yang, A., Wang, Z., Bunting, K.D., Davuluri, G., Green, M.R., and Devireddy, L.R. (2011). Multiple apoptotic defects in hematopoietic cells from mice lacking lipocalin 24p3. *J Biol Chem* 286**,** 20606-20614.

Lozoff, B., and Georgieff, M.K. (2006). Iron deficiency and brain development. *Semin Pediatr Neurol* 13**,** 158-165.

Macmanus, J.P., Graber, T., Luebbert, C., Preston, E., Rasquinha, I., Smith, B., and Webster, J. (2004). Translation-state analysis of gene expression in mouse brain after focal ischemia. *J Cereb Blood Flow Metab* 24**,** 657-667.

Marques, F., Falcao, A.M., Sousa, J.C., Coppola, G., Geschwind, D., Sousa, N., Correia-Neves, M., and Palha, J.A. (2009). Altered iron metabolism is part of the choroid plexus response to peripheral inflammation. *Endocrinology* 150**,** 2822-2828.

Marques, F., Rodrigues, A.J., Sousa, J.C., Coppola, G., Geschwind, D.H., Sousa, N., Correia-Neves, M., and Palha, J.A. (2008). Lipocalin 2 is a choroid plexus acute-phase protein. *J Cereb Blood Flow Metab* 28**,** 450-455.

Meheus, L. (1993). Identification by microsequencing of lipopolysaccharide-induced proteins secreted by mouse macrophages. *J Immunol* 151**,** 1535-1547.

Mesquita, A.R., Pego, J.M., Summavielle, T., Maciel, P., Almeida, O.F., and Sousa, N. (2007). Neurodevelopment milestone abnormalities in rats exposed to stress in early life. *Neuroscience* 147**,** 1022-1033.

Mesquita, S.D., Ferreira, A.C., Sousa, J.C., Santos, N.C., Correia-Neves, M., Sousa, N., Palha, J.A., and Marques, F. (2012). Modulation of iron metabolism in aging

and in Alzheimer's disease: relevance of the choroid plexus. *Front Cell Neurosci* 6**,** 1-10.

Ming, G.L., and Song, H. (2011). Adult neurogenesis in the mammalian brain: significant answers and significant questions. *Neuron* 70**,** 687-702.

Mishra, J., Mori, K., Ma, Q., Kelly, C., Barasch, J., and Devarajan, P. (2004). Neutrophil gelatinase-associated lipocalin: a novel early urinary biomarker for cisplatin nephrotoxicity. *Am J Nephrol* 24**,** 307-315.

Moos, T., Skjoerringe, T., Gosk, S., and Morgan, E.H. (2006). Brain capillary endothelial cells mediate iron transport into the brain by segregating iron from transferrin without the involvement of divalent metal transporter 1. *J Neurochem* 98**,** 1946-1958.

Mori, K., Lee, H.T., Rapoport, D., Drexler, I.R., Foster, K., Yang, J., Schmidt-Ott, K.M., Chen, X., Li, J.Y., Weiss, S., Mishra, J., Cheema, F.H., Markowitz, G., Suganami, T., Sawai, K., Mukoyama, M., Kunis, C., D'agati, V., Devarajan, P., and Barasch, J. (2005). Endocytic delivery of lipocalin-siderophore-iron complex rescues the kidney from ischemia-reperfusion injury. *J Clin Invest* 115**,** 610-621.

Morris, R. (1984). Developments of a water-maze procedure for studying spatial learning in the rat. *J Neurosci Methods* 11**,** 47-60.

Mucha, M., Skrzypiec, A.E., Schiavon, E., Attwood, B.K., Kucerova, E., and Pawlak, R. (2011). Lipocalin-2 controls neuronal excitability and anxiety by regulating dendritic spine formation and maturation. *Proc Natl Acad Sci U S A* 108**,** 18436-18441.

Nairz, M., Theurl, I., Schroll, A., Theurl, M., Fritsche, G., Lindner, E., Seifert, M., Crouch, M.-L.V., Hantke, K., Akira, S., Fang, F.C., and Weiss, G. (2009). Absence of functional Hfe protects mice from invasive Salmonella enterica Serovar Typhimurium infection via induction of lipocalin-2. *Blood* 114**,** 3642–3651.

Naude, P.J., Nyakas, C., Eiden, L.E., Ait-Ali, D., Heide, R.V., Engelborghs, S., Luiten, P.G., De Deyn, P.P., Den Boer, J.A., and Eisel, U.L. (2012). Lipocalin 2: Novel component of proinflammatory signaling in Alzheimer's disease. *FASEB J* 26**,** 2811-2823.

Nelson, A., Barasch, J., Bunte, R., and Weiser, J. (2005). Bacterial colonization of nasal mucosa induces expression of siderocalin, an iron-sequestering component of innate immunity. *Cell Microbiol* 7**,** 1404–1417.

Nielsen, B.S., Borregaard, N., Bundgaard, J.R., Timshel, S., Sehested, M., and Kjeldsen, L. (1996). Induction of NGAL synthesis in epithelial cells of human colorectal neoplasia and inflammatory bowel diseases. *Gut* 38**,** 414-420.

Nilsen-Hamilton, M., Hamilton, R., and Adams, G. (1982). Rapid selective stimulation by growth factors of the incorporation by BALB/C 3T3 cells of [^{35}S] methionine into a glycoprotein and five superinducible proteins. *Biochem Biophys Res Commun* 108**,** 158-166.

Ottoni, E.B. (2000). EthoLog 2.2: a tool for the transcription and timing of behavior observation sessions. *Behav Res Methods Instrum Comput* 32**,** 446-449.

Paxinos, G., and Franklin, K.B. (2001). *The Mouse Brain in Stereotaxic Coordinates.* USA: Academic Press.

Pego, J.M., Morgado, P., Cerqueira, J.J., Almeida, O.F., and Sousa, N. (2006). Mismatch between anxiety status and morphometric parameters in the amygdala and bed nucleus of the stria terminalis. *Behav Brain Res* 173**,** 320-325.

Pego, J.M., Morgado, P., Pinto, L.G., Cerqueira, J.J., Almeida, O.F., and Sousa, N. (2008). Dissociation of the morphological correlates of stress-induced anxiety and fear. *Eur J Neurosci* 27**,** 1503-1516.

Poh, K.W., Yeo, J.F., Stohler, C.S., and Ong, W.Y. (2012). Comprehensive gene expression profiling in the prefrontal cortex links immune activation and neutrophil infiltration to antinociception. *J Neurosci* 32**,** 35-45.

Porsolt, R.D., Bertin, A., and Jalfre, M. (1977). Behavioral despair in mice: a primary screening test for antidepressants. *Arch Int Pharmacodyn Ther* 229**,** 327-336.

Prut, L., and Belzung, C. (2003). The open field as a paradigm to measure the effects of drugs on anxiety-like behaviors: a review. *Eur J Pharmacol* 463**,** 3–33.

Radley, J.J., Sisti, H.M., Hao, J., Rocher, A.B., Mccall, T., Hof, P.R., Mcewen, B.S., and Morrison, J.H. (2004). Chronic behavioral stress induces apical dendritic reorganization in pyramidal neurons of the medial prefrontal cortex. *Neuroscience* 125**,** 1-6.

Rathore, K.I., Berard, J.L., Redensek, A., Chierzi, S., Lopez-Vales, R., Santos, M., Akira, S., and David, S. (2011). Lipocalin 2 plays an immunomodulatory role and has detrimental effects after spinal cord injury. *J Neurosci* 31**,** 13412-13419.

Ratledge, C., and Dover, L. (2000). Iron metabolism in pathogenic bacteria. *Annu Rev Microbiol* 54**,** 881-941.

Richardson, D.R. (2005). 24p3 and its receptor: dawn of a new iron age? *Cell* 123**,** 1175-1177.

Romero, L.M. (2002). Seasonal changes in plasma glucocorticoid concentrations in free-living vertebrates. *Gen Comp Endocrinol* 128**,** 1-24.

Roudkenar, M.H., Halabian, R., Roushandeh, A.M., Nourani, M.R., Masroori, N., Ebrahimi, M., Nikogoftar, M., Rouhbakhsh, M., Bahmani, P., Najafabadi, A.J., and Shokrgozar, M.A. (2009). Lipocalin 2 regulation by thermal stresses: protective role of Lcn2/NGAL against cold and heat stresses. *Exp Cell Res* 315**,** 3140-3151.

Schmidt-Ott, K.M., Mori, K., Li, J.Y., Kalandadze, A., Cohen, D.J., Devarajan, P., and Barasch, J. (2007). Dual action of neutrophil gelatinase-associated lipocalin. *J Am Soc Nephrol* 18**,** 407-413.

Sengelov, H., Boulay, F., Kjeldsen, L., and Borregaard, N. (1994). Subcellular localization and translocation of the receptor for N-formylmethionyl-leucyl-phenylalanine in human neutrophils. *Biochem. J.* 299**,** 473-479.

Sholl, D.A. (1956). The measurable parameters of the cerebral cortex and their significance in its organization. *Prog Neurobiol***,** 324-333.

Silva, R., Lu, J., Wu, Y., Martins, L., Almeida, O.F., and Sousa, N. (2006). Mapping cellular gains and losses in the postnatal dentate gyrus: implications for psychiatric disorders. *Exp Neurol* 200**,** 321-331.

Sunil, V.R., Patel, K.J., Nilsen-Hamilton, M., Heck, D.E., Laskin, J.D., and Laskin, D.L. (2007). Acute endotoxemia is associated with upregulation of lipocalin 24p3/Lcn2 in lung and liver. *Exp Mol Pathol* 83**,** 177-187.

Taupin, P. (2007). BrdU immunohistochemistry for studying adult neurogenesis: Paradigms, pitfalls, limitations, and validation. *Brain Res Rev* 53**,** 198 – 214.

Thouvenot, E., Lafon-Cazal, M., Demettre, E., Jouin, P., Bockaert, J., and Marin, P. (2006). The proteomic analysis of mouse choroid plexus secretome reveals a high protein secretion capacity of choroidal epithelial cells. *Proteomics* 6**,** 5941-5952.

Unger, E.L., Paul, T., Murray-Kolb, L.E., Felt, B., Jones, B.C., and Beard, J.L. (2007). Early iron deficiency alters sensorimotor development and brain monoamines in rats. *J Nutr* 137**,** 118-124.

Uylings, H.B., Ruiz-Marcos, A., and Van Pelt, J. (1986). The metric analysis of three-dimensional dendritic tree patterns: a methodological review. *J Neurosci Methods* 18**,** 127-151.

Vaidya, V.A., Fernandes, K., and Jha, S. (2007). Regulation of adult hippocampal neurogenesis: relevance to depression. *Expert Rev Neurother* 7**,** 853-864.

Van Der Meer, M., Baumans, V., Hofhuis, F.M., Olivier, B., and Van Zutphen, B.F. (2001). Consequences of gene targeting procedures for behavioural responses and morphological development of newborn mice. *Transgenic Res* 10**,** 399-408.

Von Bohlen Und Halbach, O. (2009). Structure and function of dendritic spines within the hippocampus. *Ann Anat* 191**,** 518-531.

Vorhees, C.V., and Williams, M.T. (2006). Morris water maze: procedures for assessing spatial and related forms of learning and memory. *Nat Protoc* 1**,** 848-858.

Vyas, A., Bernal, S., and Chattarji, S. (2003). Effects of chronic stress on dendritic arborization in the central and extended amygdala. *Brain Res* 965**,** 290-294.

Walker, D.L., Toufexis, D.J., and Davis, M. (2003). Role of the bed nucleus of the stria terminalis versus the amygdala in fear, stress, and anxiety. *Eur J Pharmacol* 463**,** 199-216.

Wenk, G.L. (2004). Assessment of spatial memory using the radial arm maze and Morris water maze. *Curr Protoc Neurosci* Chapter 8**,** Unit 8 5A.

Wotjak, C. (2004). Of mice and men: potentials and caveats of behavioral experiments with mice. *Futura* 19**,** 158-169.

Wu, Z.L., Ciallella, J.R., Flood, D.G., O'kane, T.M., Bozyczko-Coyne, D., and Savage, M.J. (2006). Comparative analysis of cortical gene expression in mouse models of Alzheimer's disease. *Neurobiol Aging* 27**,** 377-386.

Yang, J., Goetz, D., Li, J.Y., Wang, W., Mori, K., Setlik, D., Du, T., Erdjument-Bromage, H., Tempst, P., Strong, R., and Barasch, J. (2002). An iron delivery pathway mediated by a lipocalin. *Mol Cell* 10**,** 1045-1056.

Yoshida, M., Goto, K., and Watanabe, S. (2001). Task-dependent strain difference of spatial learning in C57BL/6N and BALB/c mice. *Physiol Behav* 73**,** 37-42.